Probabilistic analysis of ship-bridge allisions when designing bridges

Reliability Engineering and System Safety 260 (2025) 111026

Contents lists available at ScienceDirect

Reliability Engineering and System Safety

journal homepage: www.elsevier.com/locate/ress

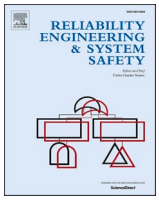

Probabilistic analysis of ship-bridge allisions when designing bridges

Axel Hörteborn [a,b,*], Jonas W. Ringsberg [b], Olov Lundbäck [a], Wengang Mao [b]

[a] RISE, Research Institutes of Sweden, Safety and Transport, Maritime Department, SE-412 58 Gothenburg, Sweden
[b] Chalmers University of Technology, Department of Mechanics and Maritime Sciences, Division of Marine Technology, SE-412 96 Gothenburg, Sweden

ARTICLE INFO

Keywords:
Monte Carlo simulation
Probabilistic analysis
Ship-bridge collision
Ship manoeuvring

ABSTRACT

The advances in civil engineering with novel bridge designs between islands and across fjords with long spans, increasing ship traffic density and larger ships in coastal areas, have resulted in an increased frequency of ship-bridge allision accidents worldwide. It is thus essential to have reliable models and methods for engineers to create safe designs of these new bridges to simulate and analyse early pro-active mitigation measures. This study presents a new ship traffic allision probabilistic simulation mid fidelity model (STAPS), which includes a ship's manoeuvrability and motion physics and uses the Monte Carlo simulation method in the probabilistic calculations. It is compared with the low fidelity model IWRAP Mk2, which is used to analyse the risk of ship allisions with structures. Two case studies with ship-allision scenarios are presented to compare how the model fidelity levels of STAPS and IWRAP Mk2 affect the calculated probability levels of ship-bridge allision events. On a general level, the results show that IWRAP Mk2 overestimates the accident probability, for example IWRAP Mk2 predicts a 4.5 times higher probability of allisions compared to STAPS in the base case, and that the failure's duration and route layouts significantly influence both models. The study concludes that IWRAP Mk2 is preferred in the early phase of bridge design and STAPS is preferred in later stages.

1. Introduction

Allision is the term used for ship accidents when a ship in motion strikes a stationary object in the ocean close to shore or offshore, such as a bridge [1]. The probability of ship-bridge allisions has increased [2,3] mainly due to two factors: increased shipping traffic and density close to shore [4], and new bridge constructions close to shore in navigational waters [3]. Human errors, especially navigational errors, are the most frequent root causes of these accidents [5–9]. The consequences of a ship-bridge allision are a combination of fatalities, destruction of infrastructure, ship damages and environmental pollution. In their study, Zhang et al. [10] identified 29 major allision accidents that occurred worldwide between January 2018 and March 2024. Two examples of severe ship-bridge allision accidents that occurred in 2024 are the Francis Scott Key Bridge in the USA [11] and the Lixinsha Bridge in China [12]. These recent allision accidents and their consequences actualise the need for ship-bridge allision probability assessments. Furthermore, understanding similar accidents and the possibility to simulate failure events, can also provide valuable insights for improving safety and reliability in other engineering domains.

The research presented in the 1970s on ship collision probabilities by Fujii et al. [13] and Macduff [14] have been important pillars in various numerical simulation and analysis methods [15], as well as in bridge building codes such as the Eurocode [16] and the AASTHO [17]. One of the largest challenges, however, is how to estimate the probability of an allision event; multiple factors must be considered, each of which might be the cause of the allision [18–22]. Methods of different fidelity levels have been proposed in the literature to simulate and analyse the probability of ship-bridge allisions. One low-fidelity model commonly used by maritime authorities is IWRAP Mk2 [23–27]. Developed based on Pedersen's [28] research, it is a geometric maritime traffic risk model originally developed for probability analysis of ship groundings and collisions [24]; the model was later extended to enable estimation of allision probability [23]. The theoretical framework for the probabilistic analysis of these events is the same as for groundings in IWRAP Mk2 [29,30]. The IWRAP Mk2 model has some limitations, e.g. it uses a static critical encounter distance and lacks support for vessel dynamics in the time domain. This has resulted in the development of more advanced models—dynamic marine transportation system (DTMS) models [31]—which are based on marine transportation system (MTS) models [32,33]. These models use Automatic Information System (AIS) data to estimate accident probability. An alternative approach to estimate accidental

* Corresponding author.
E-mail address: Axel.Horteborn@ri.se (A. Hörteborn).

https://doi.org/10.1016/j.ress.2025.111026
Received 11 November 2024; Received in revised form 1 February 2025; Accepted 11 March 2025
Available online 13 March 2025

probability is to use a combination of machine learning (ML) algorithms and known accidents [8,34–37]. Instead of using past accidents, Rong et al. [38] introduced group clustering on AIS data to define abnormal behaviour, and Korupoju et al. [39] used fuzzy logic on the AIS data to estimate the probability of ship-ship collision. Xue et al. [40] used leaky noisy-max mechanism in a Bayesian modelling to ship accidents in the Yangtze River. They concluded that with more surveillance and monitoring the accident probability could be reduced with more proactive decisions. Recently, the probability of risk of accidents involving autonomous vessels, also known as Maritime Autonomous Surface Ships (MASS), has been studied using structure-modelling, catastrophe modelling and statistical analysis [41–43]. However, none of these models have yet to be proven in the specific case of ship-bridge allisions.

The models that build on the pillars from Fujii et al. [13] and Macduff [14] are classified as low-fidelity models, which have an important practical use. They have a theoretical framework that does not require or include the ships' hydro- or aerodynamic characteristics, hence they are easy to use and considered as fast-running codes. However, the advancement of computation resources together with the advancing knowledge on how a ship's manoeuvrability is affected by varying metocean conditions have resulted in a need to move towards simulation models with higher fidelity, e.g., to execute probabilistic analysis of ship-bridge allisions. Therefore, maritime manoeuvre simulators (MMS) have been used as mid-fidelity models by several scholars, since MMS models can more realistically and accurately consider metocean and fairway conditions [44] compared to IWRAP Mk2, MTS and DMTS models. Advantages that encourage the use of MMS in ship-bridge allision simulations have been presented by various scholars [40,45–47] who have argued that its ability to simulate safe manoeuvring is an important part of determining accident probability and developing avoidance strategies and determining the probability of fatigue due to the workload.

In a recent study, Hörteborn and Ringsberg [48] presented a mid-fidelity model utilising probabilistic simulations for the analysis of ship-bridge allisions. This model used a fast-running version of an MMS to reduce simulation time without compromising the accuracy of the probabilistic analyses. A novelty with the model is that it included detailed local failure statistics of ship traffic scenarios, which were concluded to be important in the comparison and assessment of mitigation actions that can reduce, among other things, the probability of allisions. The main objective of the present study is to present a new development of this model called STAPS (ship traffic allision probability using Monte Carlo simulations). AIS data, MMS, failure event statistics and the Monte Carlo simulation method are the fundamental pillars of STAPS. In addition to the work presented by Hörteborn and Ringsberg [48], STAPS has been extended to include more failure events for the probabilistic analysis of ship-bridge allision accidents. In this study, the STAPS model is compared with IWRAP Mk2 in ship-bridge allision scenarios to identify the pros and cons of their respective methodologies. Since this type of benchmarking is scarce in the literature, suggestions are presented as to when and why each of the methodologies should be used.

The remainder of the paper is organised as follows: Chapter 2 offers a brief presentation of the models IWRAP Mk2 and STAPS. Two case studies have been designed to enable one fundamental and one real-life comparison between the methodologies (hereafter referred to as models). Chapter 3 presents the two case studies, and the results from the simulations are presented in Chapter 4. Chapter 5 presents a discussion of how the results from the case studies could be utilised in a broader perspective, i.e., when and why each model should be used in the design of new bridges. The conclusions of the study are presented in Chapter 6.

2. Models and methods

There are a variety of causes that can lead to a ship-bridge allision. According to Čorić et al. [15], the most common categorisation of the causes of a ship-bridge allision is the list proposed by Pedersen et al. [28,49]; see Fig. 1 for an illustration.

I. The ship follows the intended route, but it has a too large offset from the route centre.
II. The ship fails to turn at a given planned turning point.
III. The ship makes an evasive action, e.g. due to encountering another ship.
IV. All other track patterns that relate to the lack of manoeuvrability of the ship, e.g. a drifting ship due to blackout.

IWRAP Mk2 and STAPS can be used to simulate and analyse all the categories except for category III. Chapters 2.2 and 2.3 present in more detail how the failure events considered by the two models differ and how they relate to accident categories I, II and IV. These descriptions are made as an introduction to the model-to-model benchmark presented in Chapter 2.3.

2.1. Processing of AIS data

The ship traffic used in both the IWRAP Mk2 software and the STAPS model relies on AIS data. Commercial ships send dynamic AIS information every few seconds and static information every 5 min [50]. To handle the large amount of data, the dynamic information (point data) is translated into trajectories using a compression algorithm similar to the Top-Down Kinematic Compression algorithm presented by Guo et al. [51]. A major part of the "data noise" in the AIS data is filtered by converting the data points into trajectories [51]. The trajectories are used to extract the amount of traffic traveling on different routes, the distributions of ship speed (for the different ship types traveling on the different routes), and the lateral distributions of the ships on the different routes. The extraction follows the same principles as how IWRAP Mk2 determines which ships are traveling on each leg [18]. These extracted data are later used to populate the legs in STAPS and in IWRAP Mk2 using a Python script that updates the XML model.

The STAPS model also uses AIS data to detect failure probability and duration distributions. In this process, the trajectories are used to query failure candidates. The point data from these candidates are later reviewed in a manual step. The details of the model for extracting the probabilities and durations are further described in [48,52].

2.2. The IWRAP Mk2 model

The IWRAP Mk2 model is a maritime risk analysis software developed to quantify the probability of ship collisions, groundings and allisions [24,29]. In a recent study by Hörteborn [29], the sensitivity of each input parameter to IWRAP Mk2 was analysed to determine its effect on the probability of groundings and allisions. A ship-bridge allision analysis requires an analyst to define the routes, called legs (l), that the ships should follow and stationary objects (o) near the fairway. The object can be, for instance, the pylons of a bridge and the bridge girder, including its height; the ship can strike the bridge girder if the height between the water level and the bridge girder is less than the ship height.

In this study, IWRAP Mk2 is run to compute powered (categories I and II) and drifting (part of category IV) ship allision accidents. The IWRAP Mk2 settings used in this study's simulations are presented in Appendix A. The probability of a ship-bridge allision in IWRAP Mk2 is calculated as the expected number of allisions per year. The ships in IWRAP Mk2 are divided into ship categories (sc) depending on their size and type. The number of allisions, N_a, is estimated as the sum of all ship categories for both powered and drifting allisions:

$$N_a = \sum_{sc=1}^{\text{no. ship categories}} \left(Ng_{p,\,sc} \times Pc_p + Ng_{d,\,sc} \times Pc_d \right) \quad (1)$$

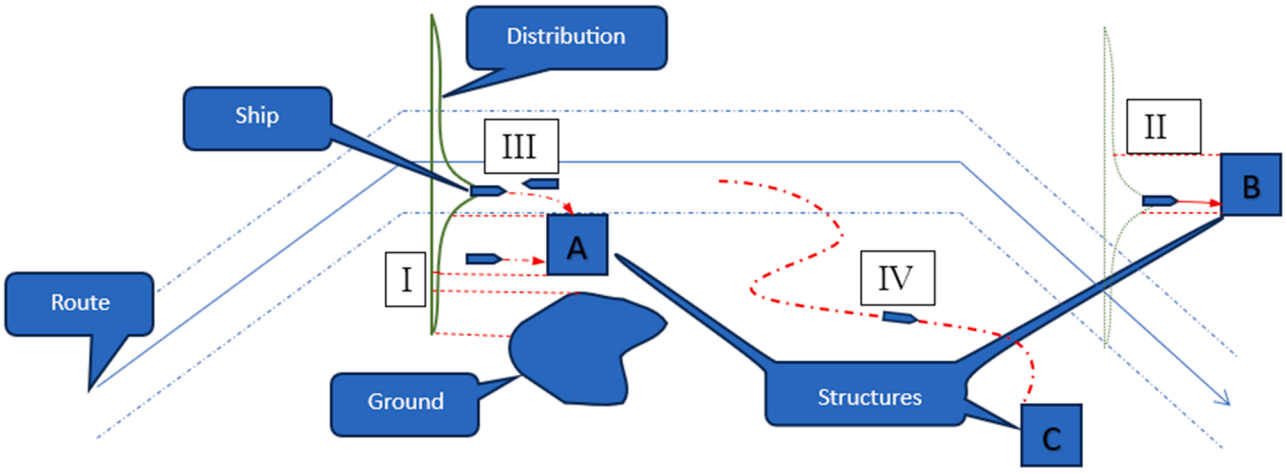

Fig. 1. Illustration of four ship incident/accident categories defined by Pedersen [28].

where $Ng_{p,sc}$ is the number of geometrical powered candidates in each ship category (presented in Chapter 2.2.1), Pc_p is the probability (causation factor) for powered accidents, $Ng_{d,sc}$ is the number of geometrical drifting candidates in each ship category (presented in Chapter 2.2.2) and Pc_d is the probability (causation factor) of the drifting accidents.

The equations presented in the following subchapters are based on the document describing the theory behind IWRAP Mk2 [24]. However, they have been slightly modified both to clarify what is included and to make them comparable to STAPS.

2.2.1. Powered accidents

A powered accident in IWRAP Mk2 refers to accident categories I and II; see Fig. 1. It defines an accident that may occur due to the ship being too far off the centre of the fairway or the ship neglecting to turn at a given required turning point. The number of powered candidates is calculated as:

$$Ng_{p,\,sc} = \sum_{o=1}^{\text{no. of objects}} \sum_{l=1}^{\text{no. of legs}} \left(N_{l,sc} e^{-\frac{d_{l(tp),\,o}}{t_m \times v_{sc}}} \int_{z_{l,o}^{min}}^{z_{l,o}^{max}} f_{l,o}(z)\mathrm{d}z \right) \tag{2}$$

where $N_{l,sc}$ is the number of ships per leg and ship category per year, $d_{l(tp),o}$ is the distance (unit: m) between the turning point of the l-th leg and the object (this distance is 0 for category I), t_m is the mean time between checks (unit: s), v_{sc} is the ship's operational speed (unit: m/s) of the ship category and $f_{l,o}(z)\mathrm{d}z$ refers to the ship's lateral distribution over each leg that overlaps with the object. Fig. 2 presents an illustration of the geometrical parameters involved in the powered accident in Eq. (2).

2.2.2. Drifting accidents

A drifting accident refers to category IV in Fig. 1. The number of drifting candidates, $N_{g,d,sc}$, is summarised in Eq. (3) as:

$$Ng_{d,\,sc} = \sum_{o=1}^{\text{no. of objects}} \sum_{l=1}^{\text{no. of legs}} \left(N_{l,sc} \times Pad_l \times Pna_{l,o} \right) \tag{3}$$

where $N_{l,sc}$ is the number of ships per leg and ship category, Pd_l is the probability of being adrift on leg l, see Eq. (4) and $Pna_{l,o}$ is the probability per leg and object that the accident cannot be avoided, see Eq. (5).

$$Pad_l = 1 - e^{-F_b \times \left(\frac{L_l}{v_{sc}}\right)} \tag{4}$$

where F_b is the blackout frequency, L_l is the length of the l-th leg and v_{sc} is the operational ship speed. The probability of the total none-

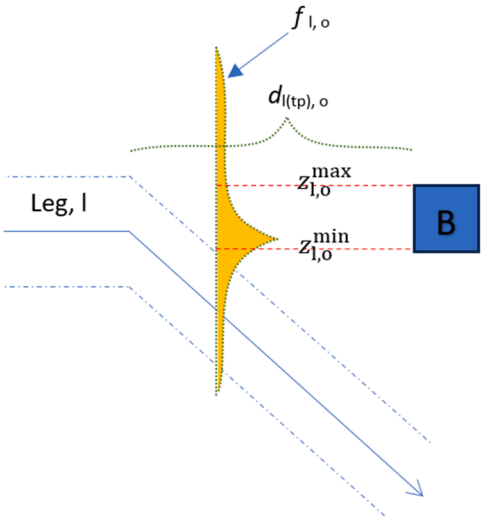

Fig. 2. An enlargement of the category II area of Fig. 1 to show the parameters involved in powered accidents.

avoidance per leg l and object o is calculated as:

$$Pna_{l,o} = \left(1 - P_{anchor}\right) \times \left(1 - Pr_{l,o}\right) \times \left(1 - Pda_{l,o}\right) \tag{5}$$

where P_{anchor} is the probability of a successful anchoring (a user-defined constant with some conditions [23]). $Pr_{l,o}$ is a user-defined function, exemplified in Appendix A, that requires the drift time between the leg and the object $Td_{l,o}$; see Eq. (7). $Pda_{l,o}$ is the probability of drifting away from an object that is calculated as a summation of the overlapping percentage of the leg and the object in eight distinct directions as:

$$Pda_{l,o} = \sum_{dir=0}^{7} Pdr_{dir\,\times\,45} \times \left(1 - \int_{z_{min}}^{z_{max}} f_{l,o,dir\times 45^\circ}(z)\mathrm{d}z \right) \tag{6}$$

where Pdr_{dir} refers to the probability of drifting into direction dir $\times$ 45° and $f_{l,o,dir\times 45^\circ}(z)\mathrm{d}z$ refers to the percentage of the leg length that covers the object in the direction dir $\times$ 45°.

$$Td_{l,o} = \frac{D_{l,o}}{V_d} \tag{7}$$

where $D_{l,o}$ is the distance between the ship's position when the drift started and the position of the allision object, and v_d is the drift speed.

IWRAP Mk2 assumes constant drift speed and that the ship's hydrodynamic characteristics are not included in the model and will therefore not affect the ship's drift. This assumption, or limitation, enables fast running and simulation times, but its influence on the results from a probabilistic analysis of a ship-allision scenario is not well established. At sea, a ship's drift speed and direction are affected by the wind, waves and current according to the ship's hydrodynamic and aerodynamic characteristics [53,54]. Models with low fidelity do not include these physics in the simulation models, while models with a higher fidelity do, e.g. the STAPS model presented in Chapter 2.3.

2.3. The STAPS model

A simulation using the STAPS model requires several steps, which are described in more detail in Hörteborn and Ringsberg [48]. The two major steps are: (i) generation of start parameters for use in an MMS and (ii) model set-up and execution of failure simulations in an MMS.

The model presented in Hörteborn and Ringsberg [48] accounted for three failure types that can result in a ship-allision accident: loss of propulsion, loss of steering and miss of turning point. Furthermore, the current study has added two more failure types to the STAPS model: wrong course at a turning point (WCT) and turn at the wrong location (TWL); see [52] for details.

The WCT and TWL failures are referred to as "active" failure types, which means that the crew decided to act at a specific point and make these turns when they were made. The former three failure types are referred to as "passive", which means that the crew was passive in their navigation. Fig. 4 shows which failure modes that can be considered in the STAPS model.

A detailed description is given in [48,52] of how AIS data are retrieved and post-processed to obtain the necessary information to determine the local frequency and duration of each of the five failure types used in the STAPS model. A brief explanation of each type is presented to clarify how they were included in a STAPS simulation.

- **Loss of propulsion:** The ship is drifting with the environment and its propeller(s) is set to 0 rpm. There is a 50/50 chance to continue using the rudder(s) to manoeuvre in a limited manner (even if some ships alter their rudder(s) during a loss of propulsion, their efficiency is decreased). Causes a category IV accident in Fig. 1.
- **Loss of steering:** The ship makes a sharp turn by setting its rudder(s) to full port/starboard and the propellers(s) to 0 rpm. Based on the studied failure it is assumed to have faulty control system and reduces its speed. Could cause a category I or IV accident in Fig. 1.
- **Miss of turning point:** The ship continues straight ahead instead of turning where required. This failure is also used for a ship that attempts to find its way back to the normal path. This is similar to category II in Fig. 1.
- **Wrong course at a turning point (WCT):** The ship turns at the correct location but sets the wrong course. Could cause a category I or IV accident in Fig. 1.
- **Turn at the wrong location (TWL):** The ship makes an active turn at a location that puts it at risk of an accident. Could cause a category I or IV accident in Fig. 1.

These failures become different failure modes in the simulations. These simulations contain a tempospatial world model and a vessel model. The vessel model is generally described by its hydrodynamic coefficients, but it also contains information regarding the vessel's speed and failure characteristics (such as its duration and turn angles). The tempospatial world model describes the geometrical layout of the scenario to be studied, including the legs (which describe the traffic paths), water depth and objects such as structures and islands. Statistical metocean data regarding winds and waves are also connected to this model. For areas and studies where waves need to be considered, they can also be included. However, in the current study, wave loads were not considered since IWRAP Mk2 cannot account for wave loads, and the real-world case scenario is located in a fjord where the influence of wave loads is minor and can be disregarded.

The parameters used in a simulation are single values. They can either be deterministic (d) or randomly generated from their respective distributions using the Monte Carlo method (mc); see Fig. 3.

The STAPS model has three deterministic parameters marked with "d" in Fig. 3: the failure type, the vessel type and the leg. They are combined into a simulation *set* in a STAPS simulation. Each simulation in all simulation sets needs to have a collection of single values for all parameters. The parameters marked with "mc" in Fig. 3 (vessel speed, failure duration, set angle deviation, lateral offset, wind speed, wind direction, current speed and current direction) are single values drawn from their respective distributions in a Monte Carlo simulation, whereas the deterministic parameters are constants in each simulation set. Two of the failure types (miss of turning point and WCT) are initiated prior to the turning points, while the other failure types are set to occur at an equal distance between each other. For these other failure types, the number of simulations to run in one set, $N^{\text{sim}}_{\text{ft,sc,l}}$, is estimated by:

$$N^{\text{sim}}_{\text{ft, sc,l}} = N_{\text{l,sc}} \times P_{\text{ft}} \times \left(\frac{L_{\text{l}}}{v_{\text{sc}}}\right) \times Y_{\text{rep}} \tag{8}$$

Here, P_{ft} is the failure probability per hour (unique for each failure type) and Y_{rep} is the number of repetitions of one year's traffic the simulation set represents. The distance along the route between the starting positions equals $N^{\text{sim}}/\, L_{\text{l}}$.

For failures that occur at planned turns, the number of simulations, $M^{\text{sim}}_{\text{ft,sc,l}}$, is estimated by Eq. (9) as:

$$M^{\text{sim}}_{\text{ft, sc,l}} = N_{\text{l,sc}} \times P_{\text{ft}} \times N_{\text{turns,l}} \times Y_{\text{rep}} \tag{9}$$

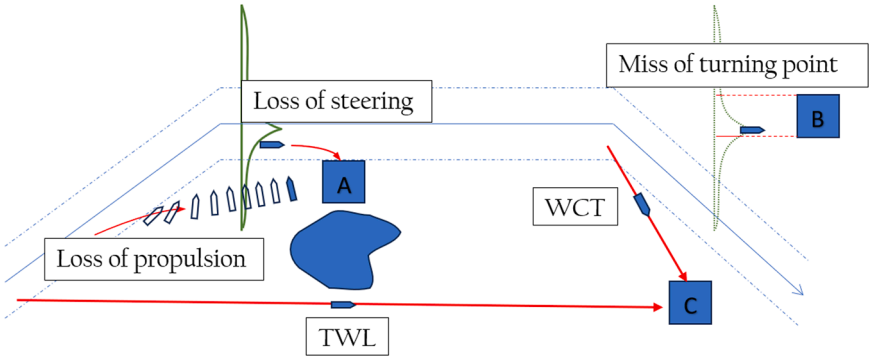

Fig. 4. Examples of a sailing fairway, passing one island and three structures (A, B and C). Paths of the five failure types are included to illustrate how each could result in an allision.

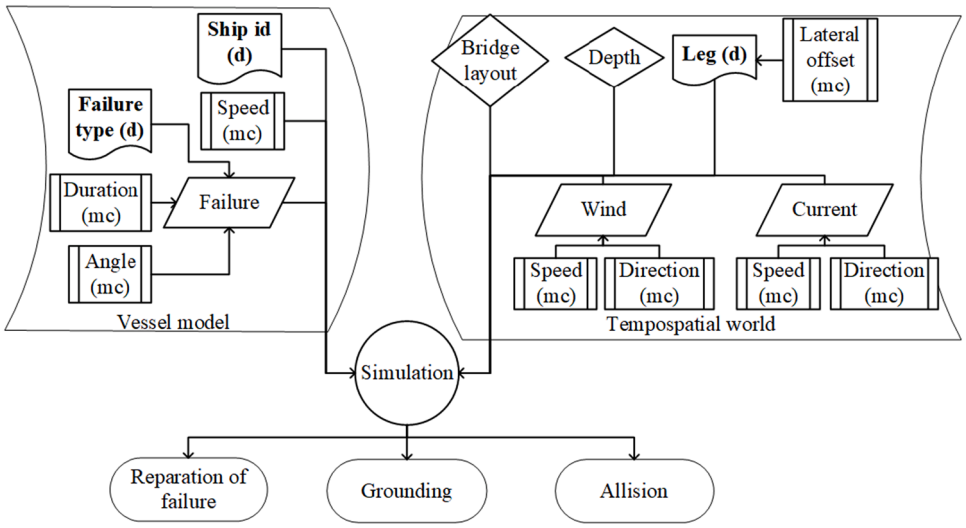

Fig. 3. Overview of parameters included in the simulation, including their type: "mc" indicates that this parameter will be randomly selected from a distribution and "d" indicates that this is a deterministic parameter. A simulation has three possible outcomes: either the simulation time runs out (the failure is repaired), the vessel grounds, or it strikes a bridge in an allision.

where $N_{\text{turns,l}}$ is the number of turns per leg.

The STAPS model presented in this study uses the in-house code Seaman [55] for the MMS, which uses PySim to solve the equations for the seakeeping motions and manoeuvrability characteristics. Each ship has a unique hydrodynamic specification to be used in the MMS that defines the manoeuvrability characteristics of the ship. The Seaman MMS can simulate ships either in full mission, with screens surrounding in 360°, or in a desktop environment with a single computer. The simulations can be carried out in real-time or fast-time mode in the desktop environment. STAPS uses the fast-time mode, where one fast-time simulation of a 15-minute ship route takes approximately 1 second to run.

The ship's rudder and engine are controlled by an autopilot, which aims to follow a predefined route at a Monte Carlo simulated ship *speed*. Each simulation in all simulation sets has a unique set of coordinates to follow (route). This route is based on the predefined route but adjusted with the Monte Carlo simulated *lateral offset* parameter (the distributions used to generate the ship speed and lateral offset are based on AIS data). The ship's starting position is laterally moved to start on this route, and the initial ship heading is set towards its next waypoint. Each individual simulation runs for 2 min before the failure is initiated to ensure that all forces of motion are correct. For simulations with a failure relative to a planned turn (miss of turning point and WCT), the starting position is moved back to the location 2 min prior to the turning point. The ship runs for 2 min plus the failure duration. If the ship strikes a ground or a bridge, the simulation is terminated early; otherwise, it ends after the duration runs out. The failure modes are designed to operate without human intervention. However, in some situations, the crew onboard could take action to reduce the probability of allision.

The Monte Carlo simulation of input parameters creates randomness in the result. To mitigate this, $Y_{\text{rep,}}$ in Eqs. (8) and (9) could be increased. To decide what Y_{rep} is good enough, a threshold should be defined, such as the spread of "the expected number of allisions in 10^4 years" (A) between three random seeds [56] should be <5 %, as expressed in Eq. (10).

$$0.95 \leq \frac{A_i}{\frac{A_1+A_2+A_3}{3}} \leq 1.05 \text{ for } i \in \{1,2,3\} \tag{10}$$

Here, A_1 corresponds to the number of allisions with seed 1, etc.

2.4. Model comparison

The different classifications of model fidelity between the IWRAP Mk2 and STAPS models justify a benchmark, since they are both applied for the same purpose in probabilistic analyses of maritime traffic simulations and analyses. There are inevitable differences between the two models, which cannot be fully controlled or pinpointed, as well as assumptions that had to be made in the current study to enable a benchmarking of the models; see Table 1 for a summary. One of the major differences is that IWRAP Mk2 relies on previous accidents, whereas STAPS relies on previous failures. There are also many similarities, e.g. the parameter generation of the models' required start input values, which must be defined to clearly describe how the comparison was made:

- In both models, the definitions of the legs, objects, structures, bathymetry, etc., are similar.
- Both models use the same number of ships, average ship speed and lateral offset from the leg, gathered from AIS data.
- Modelling of accident category II in IWRAP Mk2 is modelled and simulated as a miss of turning point failure in STAPS.
- Modelling of drifting accident category IV in IWRAP Mk2 is modelled and simulated as a loss of propulsion failure in STAPS.
- The probability of drifting failure in IWRAP Mk2 is calculated using Eq. (3). In STAPS, the corresponding probability is calculated as $P_{\text{ft}} \times L_{\text{l}} / v_{\text{sc}}$ as part of Eq. (8).
- The duration of a failure in the STAPS model is based on AIS data analyses. Hence, it includes both $P_{\text{anchor,l}}$ and $P_{\text{repaired,l,o}}$ in Eq. (6). In STAPS, the term $P_{\text{drift away,l,o}}$ is considered by the model's capability of considering the interaction between metocean conditions and the ship's hydrodynamic characteristics.

3. Benchmark using case studies

Two case studies were designed to benchmark the two models for different situations, considering the complexity of the simulated case. The first case study is a low-level case with well-defined ship-bridge allision scenarios and clear metocean conditions. Its primary purpose is to compare how IWRAP Mk2 simplifications of the ship behaviour affect the estimated allision probability. The second case study is a high-level case based on a real-world situation for estimating the ship-bridge allision probability in the design of a new bridge across a fjord in Norway.

Table 1
Examples of important differences in the IWRAP Mk2 and STAPS models in ship-bridge allision analysis.

Topic	IWRAP Mk2	STAPS
Modelling of ship movements	Statistical model of how the traffic on an entire leg is homogeneously moving. Actual ship movements are not simulated; instead, the probability of allision is instead computed based on geometric distributions.	Each ship is simulated individually, the ship following the legs until a failure is initiated. During the entire simulation, the ship is affected by the hydrodynamic physics.
Modelling of active navigational errors.	A "fake leg" can be introduced in the model with 1–2 % of the traffic intended to pass in the navigational span in a uniform distribution spanning the entire bridge length; see [49,57], who introduced the "fake leg".	Can be modelled as TWL and WCT failures.
Modelling of loss of steering failure.	Cannot be simulated by IWRAP.	Can be modelled as loss of steering.
Influence on ship drift from metocean conditions.	Simplified model: based on area specific information the analyst defines one constant drift speed and eight pre-defined drift directions shown in Fig. 5. Probabilities are calculated according to Eqs. (4) and (5).	The weather is randomly selected for each simulation and its influence is computed by the MMS. Thus, unique for each ship type (vessel model) and includes all metocean conditions.
Modelling of the start speed and direction of a drifting failure.	The ship continues along the path of the leg when the drift failure occurred, with a speed corresponding to the speed at the instant when the drift was initiated.	The leg heading is used as the start direction. The simulation starts with the operational speed of the ship (which is a Monte Carlo simulated input parameter). The ship speed and the drift direction changes with time depending on the metocean conditions and the ship's aero- and hydrodynamic characteristics.

In this case study, the complexity of the analysis case is more extensive compared to the former, considering the definition of multiple legs, type of failure events, modelling of metocean conditions and number of ship models used in the analysis. The results from the two case studies will form the basis for a discussion about the pros and cons of the two models.

3.1. Case study 1: simulation of one bridge with one leg

Four simplistic scenarios were designed to highlight fundamental differences between the IWRAP Mk2 and STAPS models. Each scenario consisted of a 1000-meter leg and was run three times with a 1000-meter-long bridge at three different offsets. The bridge was lower than the ship, i.e. the ship could not pass under it. Annual ship traffic is defined as 1000 ships of a single ship type in both directions of the leg, where the ships operate at an average speed of 15 knots. The probability of drifting ($P_{\text{ft=loss of propulsion}}$) was set to the default blackout frequency of 0.75 per year.

Three scenarios, 1.1 to 1.3, were designed to simulate drifting failure events by options of controlling drift directions and initial speed when the failure was initiated. Scenario 1.4 was designed to simulate the powered accident category II in Fig. 1, the miss of turning point in Fig. 4. The settings used in IWRAP Mk2 are presented in Appendix A.

- **Scenario 1.1: limited drift direction and limited start speed**

The drift/current directions were equally divided into eight distinct directions in both models; see Fig. 5. The drift speed was set to 1 knot in IWRAP Mk2, and the ships speed (perpendicular to the ship heading) and current speed set to 1 knot in STAPS to make it as similar as possible between the models. This scenario should be regarded as the base case in comparison to Scenarios 1.2 and 1.3 for STAPS. No modifications were made in the IWRAP Mk2 model in these two scenarios.

- **Scenario 1.2: unlimited drift direction in STAPS but limited start speed**

The same settings as in Scenario 1.1, but in this scenario, STAPS was not restricted to distinct drifting directions (a change that is not possible in the IWRAP Mk2 software). This quantified the effect of the limitation of distinct drifting directions (with this scenario geometry).

- **Scenario 1.3: unlimited drift direction and unlimited start speed in STAPS**

The same settings as Scenario 1.1, but in this scenario, STAPS was not restricted to distinct drifting directions or 1 knot starting speed (a change that is not possible in the IWRAP Mk2 software). The ships simulated in STAPS used the same start heading as leg direction and were initiated without propulsion in with 15 knots (and 1 knot current speed evenly distributed).

- **Scenario 1.4: powered accident**

In this scenario, the leg was rotated 90° and directly pointed at the bridge, ensuring that the ships that failed to turn would strike the bridge at full speed. This scenario highlighted that powered accidents due to missed turns were estimated in similar manners in both models.

Each scenario was run 9 times; using 3 different distances between the leg and the bridge, 1, 3, respective 5 nautical miles; and using 3 different models: one IWRAP Mk2 model and two STAPS models with two different ship types. As mentioned above, two STAPS models were included to illustrate how different ship categories (the hydrodynamic effects) affect the allision probability, an effect IWRAP Mk2 cannot

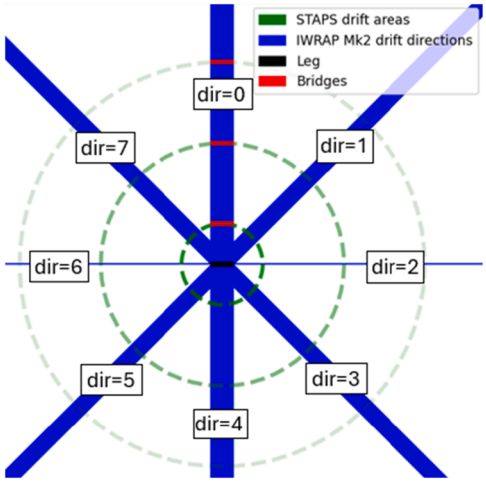

Fig. 5. The three (red) bridges and the leg (black) in Scenarios 1.1 to 1.3. The blue areas indicate where ships may drift from a 1000-meter-long leg in IWRAP Mk2 (dir[0–7] × 45°). The ships may drift in any direction in STAPS (except in Scenario 1.1). The transparency of the green circles indicates the decreasing proportion that the bridge length has on the total circumference.

consider. The two ship categories were represented by a bulk carrier with a length over all (LOA) of 90 m and a container ship with LOA 225 m.

In all the scenarios, wave and wind loads were set to zero in STAPS. However, ocean current was included in the STAPS model to simulate the loss of propulsion failure trying to mimic the conditions in IWRAP Mk2. To obtain a drifting behaviour in STAPS that was as similar as possible to IWRAP Mk2 in Scenario 1.1, the start heading was turned perpendicular to the current direction (instead of using the leg direction as heading).

The eight directions that a west-east 1000-meter-long leg can drift in IWRAP Mk2 are illustrated with blue in Fig. 5 (i.e. there will be no accidents outside the blue areas in IWRAP Mk2). In STAPS, a ship can drift in any direction as illustrated by the green circles. As the size of these circles increases, the proportion of the circle's circumference representing the bridge decreases, illustrated by the transparency of the green colour.

Both models are using the example values presented in Appendix A. However, STAPS runs the failure simulation for a duration of time, which may be regarded as an inverse of the repair time function. The repair time function in Appendix A Eq. (A-1) (for drifting accidents) and Eq. (2) (for powered accidents) are rewritten as Eq. (11) and (12) to obtain how many seconds (T_d *drifting time* and T_p *powered time)* to run the simulation for.

$$T_d = 3600 \times \left(\frac{\ln(1 - P_{\text{rnd}})}{1.05}\right)^{1\!0.9} \tag{11}$$

$$T_p = -180 \times \ln(P_{\text{rnd}}) \tag{12}$$

where P_{rnd} is a random value from a uniform distribution [0,1].

3.2. Case study 2: simulation of a real-world scenario

This study consists of a realistic scenario including multiple legs, shallow areas, different types of vessels, the annual dominant current and wind directions in the area and additional types of failures to represent a realistic probabilistic analysis. The area and its characteristics are described in the first subchapters and the scenarios are presented in Chapter 3.2.4.

3.2.1. Description of topology, fairway and ship traffic

A new bridge over Halsafjorden (Norway) was selected as the realistic example in this case study. It is located on the west coast of Norway between Bergen and Trondheim; see Fig. 6. The fjord is approximately 2000 meters wide and 400 meters deep, making it impossible to anchor to avoid allisions. Fig. 6 also shows the fjord's layout, including a new planned bridge (blue line), AIS tracks (red lines) of today's ship traffic and three legs marked as red solid lines that indicate how future ship traffic is planned if the bridge is built. The AIS tracks used for the traffic analysis were based on the ship traffic in the area during year 2023.

Before the bridge is built, the ship traffic in the area is dominated by ferries that cross the fjord; see the red ellipsoid of AIS tracks in Fig. 6. When the bridge has been built, there is no longer a need to have ferry traffic and supply ships for bunkering, hence these vessels were removed from this case study's simulations. The remaining ship traffic in the case study is presented in Table 2 as 7 ship categories navigating on 3 routes. Route 1 passes outside the fjord, Route 2 goes to/from the northwest, and Route 3 goes to/from the northeast; see Fig. 6 (right).

The new floating bridge across the fjord will have a 370-meter-wide navigational span at the west part of the bridge; see Fig. 7 for the IWRAP Mk2 model layout (the same geometry is also used in STAPS). Fig. 7 shows the legs: Route 1 in Table 3 is defined by LEG 6; Route 2 by LEGs 2, 5 and 7; while Route 3 is defined by LEGs 3, 7 and 17. Table 1 in Chapter 2.3 displayed that active navigational errors in IWRAP Mk2 need to be modelled by a fake leg. This leg is shown in Fig. 7 as LEG 20. It is in the centre of the fjord's span and contains 2 % (as suggested by Pedersen et al. [49]) of the original ship traffic on LEG 7. This entails that Routes 2 and 3 are computed with 98 % of the ship traffic.

3.2.2. Environmental statistics

The wind data for the area were sampled from the Norwegian

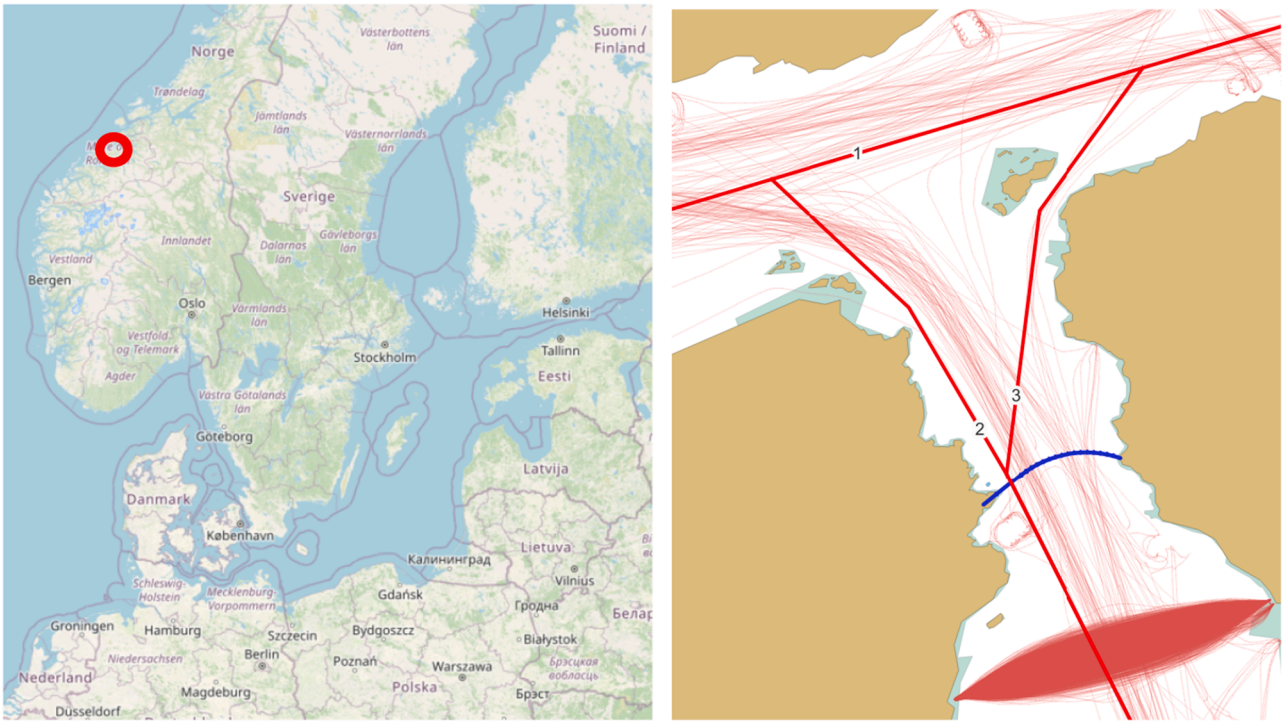

Fig. 6. (Left) Overview map, the red ring indicates where the Halsafjorden is located in Norway. (Right) The ship traffic (red) in the Halsafjorden during June 2023, including legs and the new bridge (blue) layout.

Table 2
Summary of the ships included in the case study; LOA is the length of the ship.

Ship category	Properties			Ships per year in both directions		
	Mean LOA (m)	Mean speed (kts)	Mean displacement (tonnes)	Route 1	Route 2	Route 3
Cargo ship 1	40	9.1	918	150	68	12
Cargo ship 2	65	10.2	2641	200	70	15
Cargo ship 3	90	9.7	5043	300	137	5
Cargo ship 4	115	11.0	8019	310	308	0
Supply ship 1	110	12	10,100	2	2	0
Supply ship 2	160	10	20,163	1	2	0
High speed vessel	40	31.8	556	100	0	0

Meteorological Institute [58], and statistics between 2015 and 01–01 and 2021–12–31 are presented as a polar plot in Fig. 8 (left). The ocean current statistics at 1 m water depth are obtained from Knutsen and Stefanakos [59]; see Fig. 8 (right). Wave statistics were also collected, and it showed that, because the fjord is relatively sheltered, the waves' influence on the ship traffic and the vessel models in STAPS were considered minor and therefore disregarded in the case study.

The wind speed polar plot in Fig. 8 shows that westbound winds dominate and northbound winds are relatively rare. The ocean current polar plot shows a relatively stable ocean current in the range of 0 to 0.6 m/s (0 to 1.2 knots). From these statistics, the ship drift speed in IWRAP Mk2 was set to 1 knot. However, its direction was re-calculated to the drift polar plot in Fig. 9 to represent ship drift from both the wind and

Table 3
Base case values for the failure statistics in Case Study 2. Here, 1.17×10^{-4} corresponds to 1.03 blackouts per year. The values are given per hour, except for those marked with *, which are defined per turn. IWRAP Mk2 uses these probabilities in Eqs. (1) to (3) and STAPS in Eqs. (8) and (9).

Failure type	Probability		Repair time (hours)	
	IWRAP Mk2	STAPS (P_{ft})	IWRAP Mk2	STAPS (T_{ft})
Loss of propulsion	$F_b = 1.17 \times 10^{-4}$	1.17×10^{-4}	Lognormal (7.63, 0.077)	Lognormal (7.63, 0.077)
Loss of steering	n/a	0.21×10^{-4}	n/a	Lognormal (7.63, 0.077)
Miss of turning point	$Pc_p = 1.55 \times 10^{-4*}$	$1.55 \times 10^{-4*}$	Eq. (2), with 180 s	Normal (360, 54)
WCT	n/a	$1.30 \times 10^{-4*}$	n/a	Lognormal (4.8, 0.70)
TWL	n/a	0.47×10^{-4}	n/a	Lognormal (4.3, 0.41)
Uniform ("fake leg")	$0.02 \times 1.55 \cdot 10^{-4}$	n/a	n/a	n/a

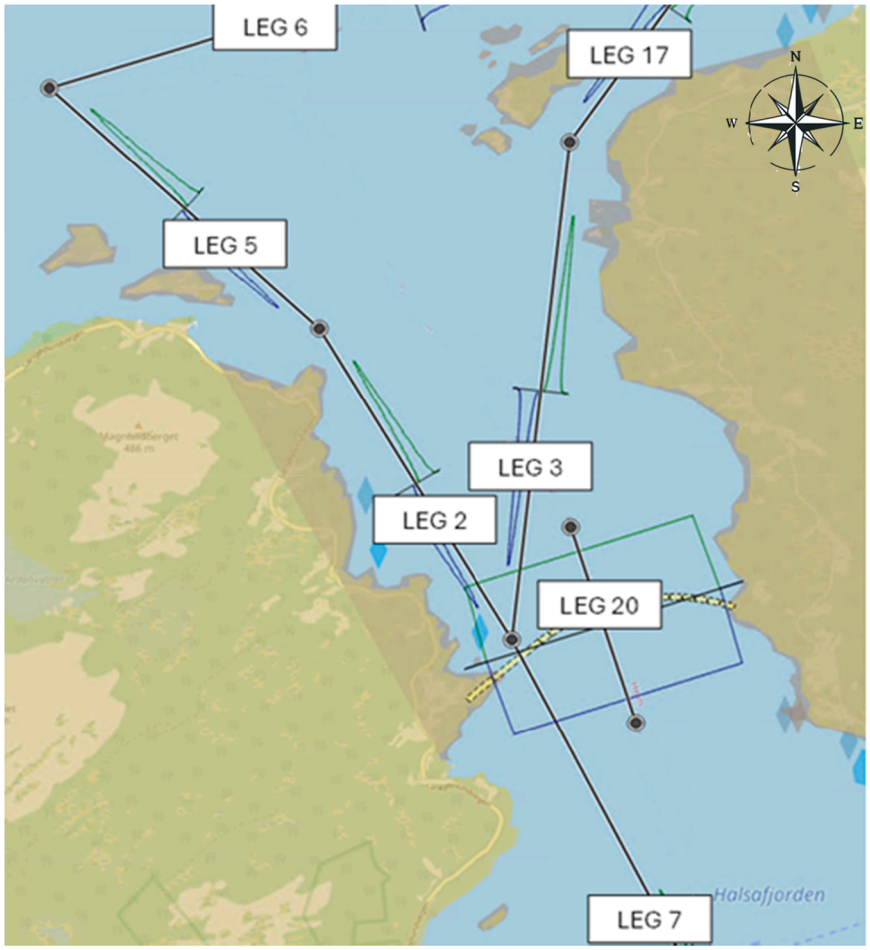

Fig. 7. The IWRAP MK2 geometrical model of the case study area, including all the legs (black solid lines) needed to run the IWRAP Mk2 and STAPS models, the green and blue illustrates the lateral offset distributions for all legs, which is normal for all legs except LEG 20 which is uniform distributed.

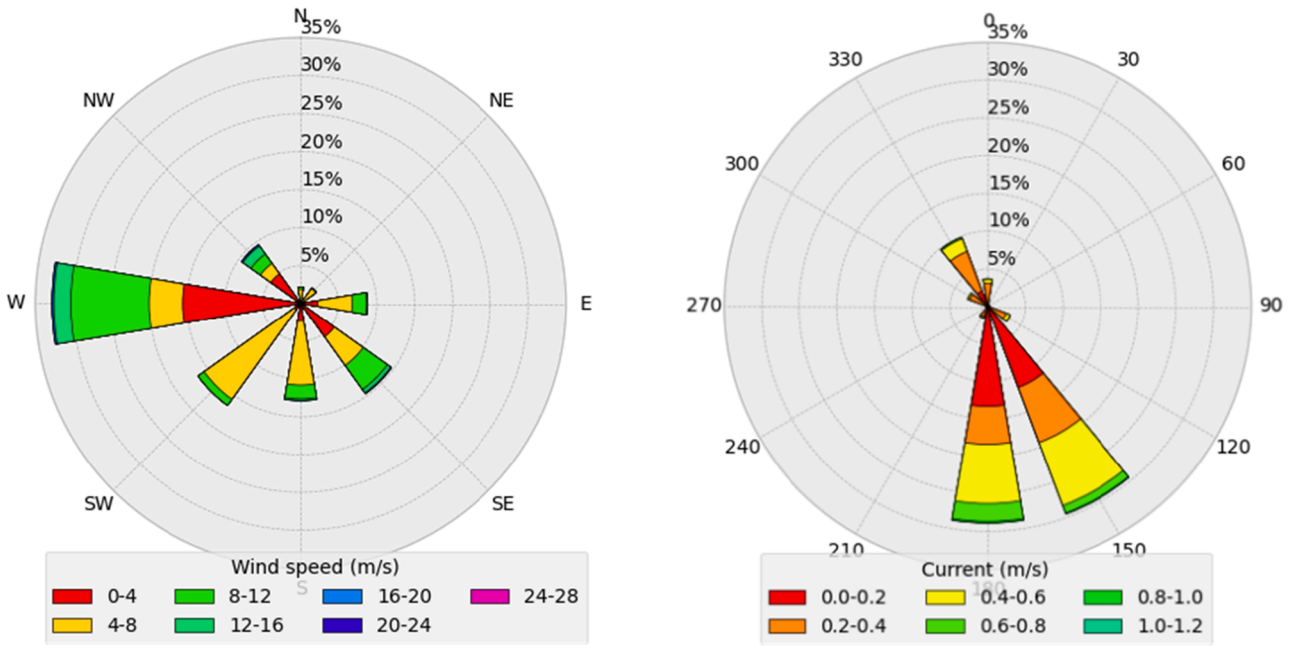

Fig. 8. (Left) Polar plot of the wind speed, describing where the wind is blowing from, based on an average of 10 min of data from Halsanestet during the years 2015–2021. (Right) Polar plot of the current speed, describing where the current is travelling to, based on statistics from *Halsafjorden middle* from 2017 to 2021.

the ocean current.

3.2.3. Failures statistics and repair times

AIS data between 2017-01-01 to 2021-12-31 were collected and post-processed in Halsafjorden and the surrounding fjords, using the methods described in Hörteborn and Ringsberg [48] and Hörteborn and Eidem [52] to find failures and calculate failure probabilities. The AIS data were used to analyse the frequency of the five failure types: blackout/loss of propulsion, loss of steering, miss of turning point, WCT and TWL. Almost all ships included in this analysis were cargo ships and tankers (AIS type 70–89).

The AIS ship traffic consisted of 420,600 ship hours in the area and 34,000 distinct turns identified at six locations. In total, 63 failures were identified: 50 loss of propulsion, 9 loss of steering, 2 miss of turning point, 2 TWL failures and no WCT failures. This corresponds to a probability of 1.17×10^{-4} per hour for a loss of propulsion/drifting ship, 2.1×10^{-5} per hour for loss of steering, 5.9×10^{-5} per turn for miss of turning point and 4.8×10^{-6} per hour for the TWL failure. It is important to mention that ship traffic patterns change when a bridge limits the fairway, hence it is recommended to use marine traffic and failure statistics from other similar areas that can be used as relatively representative values in the STAPS model; see examples of passive failure probabilities in the Great Belt area, Denmark [21,42,46] and active failure probabilities [52]. Since no WCT failures were found in the studied area, the probability and duration from a larger area close by with similar prerequisites as in Hörteborn and Eidem [52] were used.

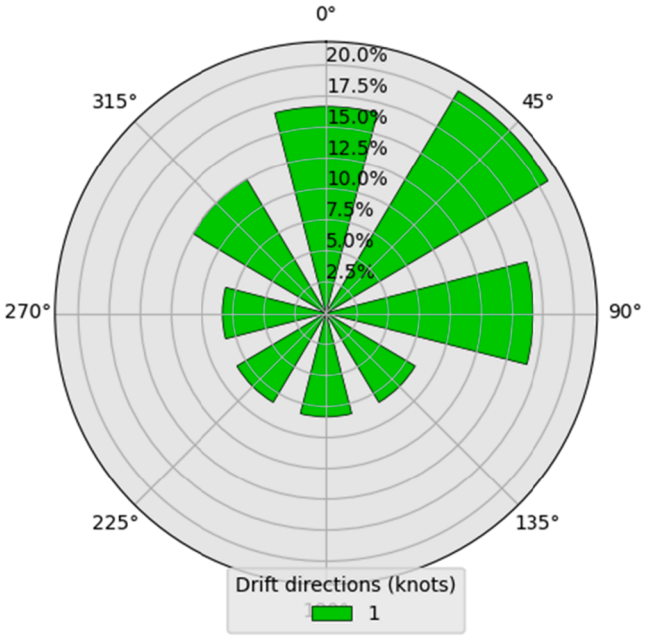

Fig. 9. Ship drift polar plot used in the IWRAP Mk2 model, the drift speed is fixed 1 knot.

The duration (T_{ft}) of the found failures were fitted to a lognormal distribution as described by Limpert et al. [60]:

$$T_{ft} = \frac{1}{\sigma x \sqrt{2\pi}} e^{\left(-\frac{(\ln(x)-\mu)^2}{2\sigma^2}\right)} \tag{13}$$

where μ is the exponent of the mean and σ is the standard deviation of the normally distributed logarithm of the variable. Based on the 59 failures in the area, the duration of loss of propulsion and loss of steering failures are described by Eq. (13) in seconds using $\mu = 7.630$ and $\sigma = 0.077$ (mean time of 34 min). For the miss of turning point, results from the Great Belt area [35] were used where the repair time was described with a normal distribution in seconds with $\mu = 360$ and $\sigma = 54$ (mean time of 6 min). The areas where the duration of WCT and TWL duration were found in Hörteborn and Eidem [52] were more open compared to the Halsafjorden; therefore, they were reduced in this study. The WCT duration was assumed with a lognormal repair time in seconds with $\mu = 4.8$ and $\sigma = 0.7$ (mean time of 2 min) and the TWL was assumed with a lognormal repair time in seconds with $\mu = 4.30$ and $\sigma = 0.41$ (mean time of 1.5 min). These values were used as the base case in Case Study 2; see Table 3 for a summary of all the probabilities and durations used in IWRAP Mk2 and STAPS.

3.2.4. Definition of simulation scenarios

Four scenarios were designed, where Scenario 2.1 is the baseline case with the primary purpose of benchmarking the IWRAP Mk2 and STAPS models for more realistic scenarios compared to Case Study 1 presented in Chapter 3.1. Scenarios 2.2 to 2.4 can be seen as parametric, sensitivity and mitigation action studies.

- **Scenario 2.1: baseline case**

  This scenario used the model settings presented in the Chapters 3.1 to 3.3.

- **Scenario 2.2: without active navigational errors**

  In this scenario, the same model setting as in Scenario 2.1 was used, except that the probability of the WCT and TWL were set to zero in STAPS, LEG 20 was removed and 100 % of the ship traffic was assumed on the other legs in IWRAP Mk2.

- **Scenario 2.3: increased miss of turning point failure duration**

  In this scenario, the same model setting as in Scenario 2.1 was used, except that the duration of the t_m parameter in IWRAP Mk2 was increased from 180 s to 240 s, and the normal distribution in STAPS was increased to $\mu = 420$ s and $\sigma = 114$ (from $\mu = 360$ s and $\sigma = 54$).

- **Scenario 2.4: introduction of VTS and TSS**

  This scenario was based on a change of the layout of the fairway; see Fig. 10 and the probabilities/duration of active navigational errors in Table 4.

Since the active navigational errors were not present in Hörteborn and Ringsberg [48], it is interesting to quantify the effect of these errors in Scenario 2.2. In that previous study, it was also concluded that the duration of the missing turning point failure, investigated in Scenario 2.3, was the most crucial parameter in the Great Belt area [48]. Hence, such a scenario is included in the current study.

Table 4
Failure statistics for an area with VTS. The values are given per hour, except for WCT, marked with * that is defined per turn.

Failure type	Probability		Repair time (hours)	
	IWRAP Mk2	STAPS (P_{ft})	IWRAP Mk2	STAPS (T_{ft})
WCT	n/a	$0.13 \times 10^{-4*}$	n/a	Lognormal (3.7, 0.85)
TWL	n/a	0.37×10^{-4}	n/a	Lognormal (3.6, 0.60)
Uniform ("fake leg")	$0.01 \times 1.0 \cdot 10^{-4}$	n/a	n/a	n/a

The Traffic Separation Scheme (TSS) in Scenario 2.4, illustrated in Fig. 10, moves the traffic from northwest to continue slightly longer out in the fjord, and the traffic from northeast to continue straight until it connects to the other traffic, approximately 2 nautical miles north of the bridge. To further reduce the risk, a Vessel Traffic Service (VTS) covering the area was implemented in this scenario. The VTS will reduce the probability of accidents by providing real-time monitoring and guidance to vessels, thereby enhancing situational awareness and decision-making for navigators [61]. It was shown in Hörteborn and Eidem [52] that a VTS reduces the probability and duration of active navigational errors. The reduced failure probabilities and durations due to the presence of the TSS and VTS are presented in Table 4. The probability reduction for in IWRAP Mk2 is both lowering the traffic volume on LEG 20 from 2 % to 1 % and the causation factor from 1.6×10^{-4} to 1×10^{-4}.

4. Results

4.1. Results from case study 1

Before the computation was run in STAPS, Y_{rep} was defined using Eq. (10). For Scenarios 1.1–1.3, Y_{rep} was defined as 10^7 yielding 61,640 loss of propulsion simulations, and for Scenario 1.4, Y_{rep} was defined as 10^6

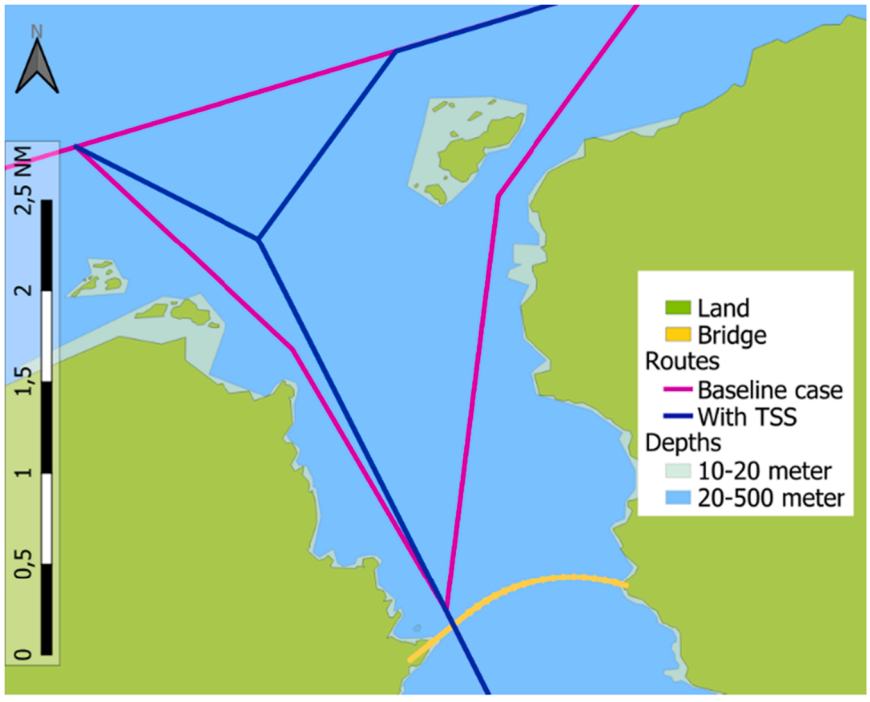

Fig. 10. The layout of the fjord with the original routes (magenta lines) and the routes with a suggested TSS (blue lines) in an enlarged view of the area north of the planned bridge (yellow line).

yielding 160,000 powered simulations, per distance and ship type.

The allision probability results for all the simulated scenarios are presented in Table 5. The scenarios are presented in the rows and the different models and distances to the bridge are presented in the columns. The different models were differently affected by the distance between the leg and the bridge. Fig. 11 presents an example of results in a bar plot from Table 5 for the case when the leg and the bridge were separated by 3 nautical miles. This distance was chosen as a representative example to illustrate the results, providing a balanced view between the shorter and longer distances of 1 and 5 nautical miles.

The results of Scenario 1.1 show that the drift probability between IWRAP Mk2 and STAPS is rather similar (note: using the "restricted" drifting conditions in STAPS). The small difference in the results is caused by the randomness in the number of "long" simulations with the northbound current that were simulated in STAPS. However, when the drifting direction was not restricted in STAPS in Scenarios 1.2 and 1.3, there was a larger difference between the IWRAP Mk2 and STAPS results. As the distance increases (see the 5 nm results), this difference between the scenarios and models also increases, which is expected since the bridge becomes a smaller part of the circle circumstance according to Fig. 5. Comparing the two different ship sizes in STAPS for Scenario 1.2 shows that the 225 m ship has a slightly higher probability of allisions compared to the 90 m ship. This difference is due to the ship geometry: the 225 m ship strikes the bridge in a slightly larger sector than the 90 m ship.

A larger difference in allision probability is observed when the initial ship speed is set to the operational speed (Scenario 1.3). This can be explained by the fact that, in this scenario, the ships travel for a longer time in the leg direction before they start to drift. The difference between the two ship types simulated in STAPS is presented in Fig. 12, which shows the paths of the two ships in a simulation with a starting speed of 15 knots. The two paths in the figure exemplify the hydrodynamic effects when the 225 m ship (blue line), having a larger mass compared to the 90 m ship, maintains its trajectory for a longer duration compared to the 90 m ship (red line), which has a smaller mass compared to the 225 m ship. The current direction was slightly different for the two ships in the simulations, since this parameter is randomly generated, and 1 of the 61,640 simulations is illustrated in the figure for each ship type. Nevertheless, the trend is similar for all randomly generated currents.

The results from Scenario 1.4, the powered allision, are almost identical between IWRAP Mk2 and STAPS (the leg in Fig. 12 is turned 90° in this scenario). The minor difference, which shows a slightly higher probability of allisions in STAPS compared to IWRAP Mk2, can be explained by how the ship geometry is modelled in the different models. In STAPS, the ship is modelled with its actual geometry, and the ship is placed with its centre of gravity at the end of the leg. This implies that the bow is approximately half of the ship's length closer to the bridge, and that the bow of the 225 m ship is closer to the bridge compared to that of the 90 m ship at the start of the simulation. The distance between the end of the leg and the bridge is used in IWRAP Mk2.

4.2. Results from case study 2

4.2.1. IWRAP Mk2: allision probability

IWRAP Mk2 is a fast-running computation code. The four scenarios took only a few seconds to run in IWRAP Mk2, since the size of the geographical area was relatively small. Table 6 presents the allision probability separated into drifting and powered allisions.

The probability of allision due to drifting was similar between Scenarios 2.1 to 2.3. For Scenario 2.4, it was lower because Route 3, defined as LEGs 3, 7 and 17 in Fig. 7, was moved away from the bridge in the new route as shown in Fig. 10.

The probability of powered allisions varied between all scenarios. Most of all powered accidents in Scenarios 2.1, 2.2 and 2.3 originated from the ships travelling southbound on LEG 5 that missed to turn in Fig. 7. The dramatic increase of accident probability in Scenario 2.3 (when t_m was increased) is further analysed in Chapter 4.2.3. The decrease in Scenario 2.4 is mainly due to the fact that ships failing to turn at LEG 5 would not strike the bridge with this layout. The difference between Scenarios 1.1 and 1.2 indicates that active navigational error accounts for 28 % of all failures in this model.

4.2.2. STAPS: allision probability

To compute the allision probability in STAPS, the number of simulations N_{sim} and M_{Sim} in Eqs. (8) and (9) must be estimated. As this requires Y_{rep}, given the Norwegian criterion [62], it should be larger than 10^4. The result of using Eq. (10) with $Y_{rep} = 10^5$ and $Y_{rep} = 10^6$ is presented in Table 7. Here, Scenario 2.2 is used, since it had the fewest simulations to run and is therefore the most sensitive.

The spread between the numbers in Table 7 presents how the randomness in the realisations of input parameters affects the number of allisions. When Y_{rep} was set to 10^5, the expected number of allisions in 10^4 years was 5.2, 6.5 and 5.5 (the first column divided by 10), which did not pass the criterion in Eq. (10). However, when Y_{rep} was increased to 10^6, the expected number of allisions in 10^4 years was 6.15, 5.89 and 5.92 (the second column divided by 100), which passed the criterion in Eq. (10).

With Y_{rep} set to 10^6 and 2.5 failures per year, approximately 2.5×10^6 simulations ($N_{sim} + M_{Sim}$) had to be run for each scenario. These scenario sets of simulations took 6 h each to run. The number of allisions caused by each failure type from the four scenarios computed by STAPS are presented in Table 8. The total probability is given as the total number of allisions divided by 10^6.

The results in Table 8 show that the number of allisions caused by loss of propulsion and loss of steering are rather constant in all four scenarios. Fig. 13 illustrates the ship paths of the allisions in Scenario 2.1 in STAPS. As shown in the figure, the largest contribution to the accident probability arises from the ships travelling south that fail to set the correct course northwest of the bridge. The exclusion of the *active navigational failures* (Scenario 2.2) decreased the number of allisions by >50 % compared to the baseline case, which indicates that they are important to consider. Similar, almost all these accidents were eliminated by introducing the TSS, moving the turning point further away; and VTS, reducing the failure probability. The large increase in accidents in Scenario 2.3 is further described and analysed in the next chapter.

4.2.3. Comparison of IWRAP Mk2 and STAPS

The yearly allision probabilities estimated for the different scenarios as determined by IWRAP Mk2 (see Table 6) and STAPS (see Table 8) are summarised in Table 9.

The results reveal some major differences in the probability of

Table 5
Probability of the different scenarios in Case Study 1. The numbers present the allision probability per year (E-1 = 1×10^{-1}).

Model	IWRAP Mk2			STAPS, 90 m ship			STAPS, 225 m ship		
Distance	1 nm	3 nm	5 nm	1 nm	3 nm	5 nm	1 nm	3 nm	5 nm
Scenario 1.1	260E-6	43E-6	8.1E-6	270E-6	47E-6	9.0E-6	270E-6	47E-6	9.0E-6
Scenario 1.2				190E-6	11E-6	1.1E-6	210E-6	13E-6	1.3E-6
Scenario 1.3				85E-6	5.4E-6	0.3E-6	2.2E-6	1.6E-6	0.6E-6
Scenario 1.4	5.9E-2	4.1E-3	2.8E-4	6.4E-2	4.1E-3	3.0E-4	6.6E-2	4.2E-3	3.2E-4

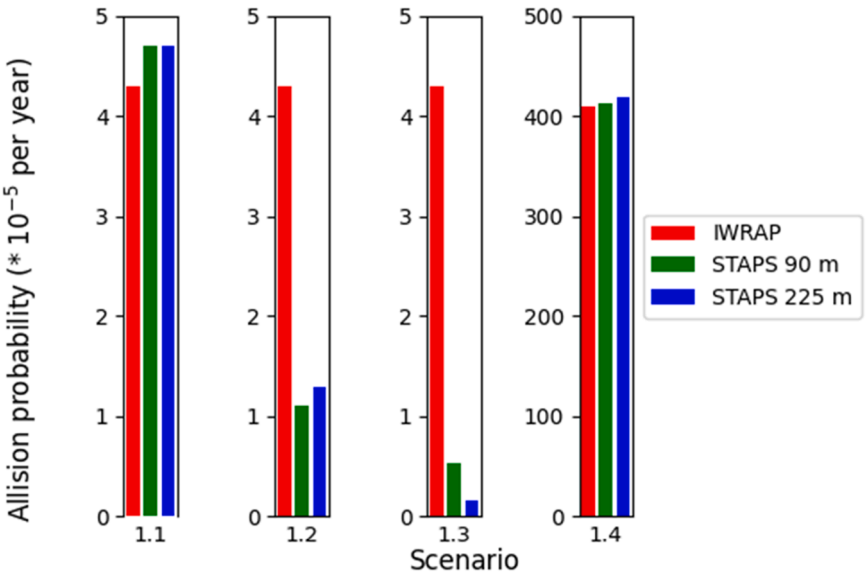

Fig. 11. The probability of allision in the four scenarios 1.1 – 1.4 (see section 3.1 for the scenario definitions) where the leg and bridge are 3 nautical miles apart.

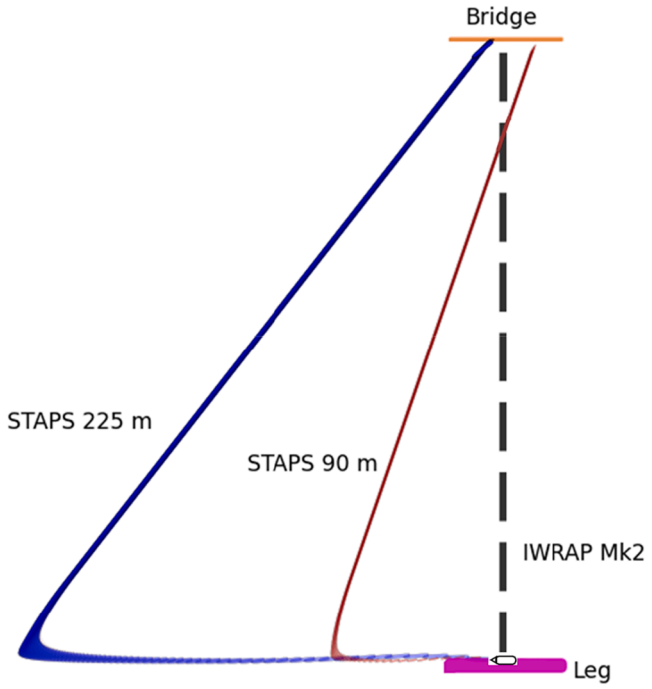

Fig. 12. Allision paths of ships striking the bridge 3 nautical miles away in Scenario 1.3. The 225 m container ship (blue) and 90 m bulk carrier ship (red) models running with an initial speed of 15 knots in STAPS; the black dashed line shows the path for these ships in IWRAP Mk2.

allision accidents between the different scenarios and the two models. IWRAP Mk2 always predicts a higher accident probability compared to STAPS. However, both models show similar trends in-between the different scenarios, i.e. an increase or decrease of allision probability related to the baseline case. They also have the same ranking in allision probability (descending magnitude): Scenario 3, 1, 2 and 4.

The number of allisions caused by ships missing a turning point is high in both models (Scenario 2.3 compared with Scenarios 2.1 and 2.2), which is explained by Fig. 14. It shows how the probability of a ship continuing to travel decreases with distance, using different failure durations. A ship travelling in 11 knots is used in the demonstration. The blue and orange lines represent the baseline case and the increased duration time in IWRAP Mk2, respectively, and the green and red lines represent the baseline case and the increased duration time in STAPS, respectively.

As illustrated by Fig. 14, the 60-second increase in duration for the missing turning point increases the probability that the failure remains at the distance to the bridge (red dashed line). A simple linear relationship between the *probability of failure remains* and the *accident probability* exists in IWRAP Mk2, i.e. a doubled increase of remaining probability equals a doubled increase of accident probability. Since the ship speed is a random parameter in STAPS, this figure is just one example, and as illustrated in Table 8, there are ships with higher speeds that will strike the bridge due to the missing turning point failure even with the base case duration.

Based on this case study, it is concluded that the difference between the two models is not primarily dependent on the model fidelity level. Instead, the difference in the results depends more on how the failures are implemented, their frequency and their duration.

5. Discussion

The two case studies compared the IWRAP Mk2 and STAPS models with different perspectives. The first study aimed at quantifying differences between the models in a controlled environment, and the second study had a wider scope where the comparison aimed at quantifying differences in a real-world probability analysis.

Scenario 1.1 in Case Study 1 illustrated that the two models could predict the same drifting probability if the behaviours of STAPS were adjusted to match the drifting conditions allowed in IWRAP Mk2. When these restrictions were removed in Scenarios 1.2 and 1.3, the case study showed some major differences with regards to how IWRAP Mk2 and STAPS estimated the probability of drifting allisions. When the enforced drifting direction was removed, the probability of drifting in the bridge's direction decreased in STAPS. However, these differences are subjected to the layout of the case study. The difference will decrease with longer legs, which is commonly used in risk assessments for larger areas. Legs not directly pointing at a drift direction will also reduce the difference between the models. Still, in certain cases, this drift behaviour can have a significant effect. For instance, when a leg points towards 0, 45, 90, 135, 180, 225, 270 or 315°, there is a "blind spot" near the end of the legs in IWRAP Mk2. The STAPS model does not have such blind spots and can also recognise that ships of different types and sizes have

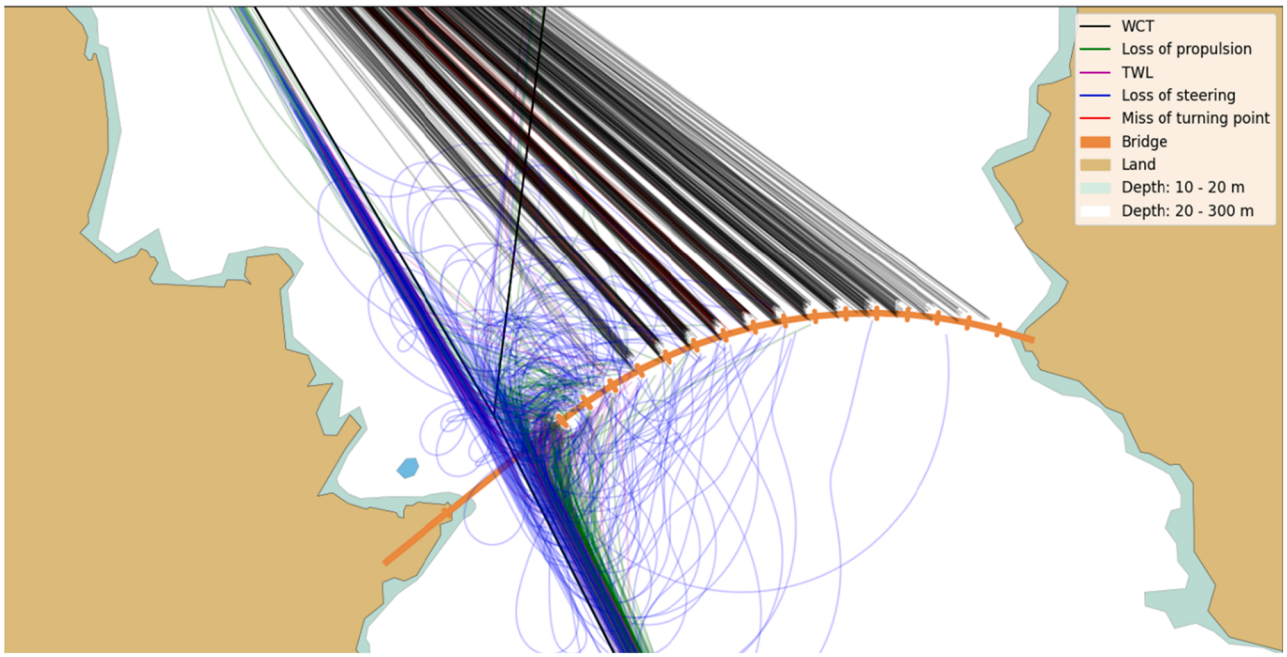

Fig. 13. Map illustrating the paths of the allision accidents from the base case. The colours indicate which type of failure led the ship to the simulated allision.

Table 6
Results of Case Study 2 computed by IWRAP Mk2 (E-1 = 1×10^{-1}).

Scenario	Probability of drifting allision	Probability of powered allision
2.1	10.8E-4	52.3E-4
2.2	10.9E-4	37.2E-4
2.3	10.8E-4	93.4E-4
2.4	9.5E-4	7.6E-4

Table 7
The number of allisions with different realisations of Scenario 2.2, using different random seeds and different numbers of yearly repetitions.

	Number of allisions with $Y_{rep} = 10^5$	Number of allisions with $Y_{rep} = 10^6$
Seed 1	52	615
Seed 2	65	589
Seed 3	55	592

Table 8
The number of allisions caused by the different failures calculated using STAPS.

Scenario	Loss of propulsion	Loss of steering	Miss of turning	WCT	TWL	Total probability
2.1	257	315	29	718	116	14.4E-4
2.2	254	324	41	0	0	6.2E-4
2.3	249	350	4493	708	107	59.1E-4
2.4	256	303	0	0	21	5.8E-4

Table 9
Summary of allision probabilities computed by IWRAP Mk2 and STAPS (E-1 = 1×10^{-1}).

	Allision probability (per year)			
Scenario	2.1	2.2	2.3	2.4
IWRAP Mk2	63.1E-4	48.1E-4	104.2E-4	16.9E-4
STAPS	14.4E-4	6.2E-4	59.1E-4	5.8E-4

different drifting patterns [63,64]. This difference affects how far away the ship will drift and thereby the probability of striking a structure. The initial speed at the time of the failure is another aspect that STAPS accounts for, as maintaining speed for a longer time has an impact on where drifting ships end up. Overall, STAPS captures these physics and where ships may end up better compared to IWRAP Mk2. However, the large difference between the results of both models in this case study depends mostly on the layout of the scenarios. Based on the first case study, two recommendations are suggested:

- Caution is needed in situations where the leg is aligned with one of the eight drift directions; the drifting cases are more "concentrated" in some directions in IWRAP Mk2 compared to real-world scenarios. Analysts should investigate if a small alteration of the leg influences the accidental probability caused by drifting ships.
- Larger ships move further away from the leg (in the leg direction) compared to smaller ships. Due to the lack of hydrodynamic equations in IWRAP Mk2, this effect is omitted, and it is therefore recommended to make the legs slightly longer in IWRAP Mk2 for critical areas.

The second case study also showed differences in the results from the two models. IWRAP Mk2 estimated a higher allision probability compared to STAPS for all scenarios, mainly due to the IWRAP Mk2's estimation of powered accidents. Therefore, one of the most important parameters to investigate is t_m in IWRAP Mk2 and the duration of missing turning point in STAPS. This has also been found in previous studies [27]. However, as illustrated in Fig. 14, the sensitivity of this parameter depends on the ship speed and the distance between the route turn and the object, indicating that the importance of the parameter will vary between different areas. For areas where the distance is shorter, the probability P_{ft} in STAPS and $P_{p,c}$ in IWRAP Mk2 might be more relevant to study in more detail in future work. Additionally, the large reduction in accident probability with the implementation of TSS/VTS in the models suggests that such measures are crucial for improving maritime safety.

Defining the models with legs and capturing data from AIS data to these legs is a similar process in both IWRAP Mk2 and STAPS. The simulation time in STAPS depends on the Y_{rep} parameter, the number

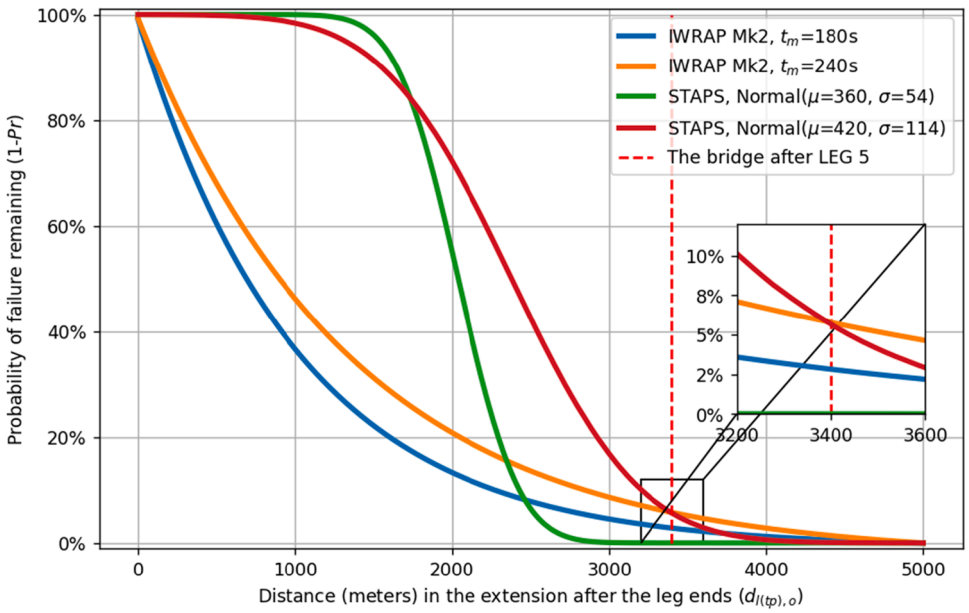

Fig. 14. The probability of failure remaining for a ship travelling in 11 knots depending on failure function. The red dotted line marks the distance between the original LEG 5 and the bridge.

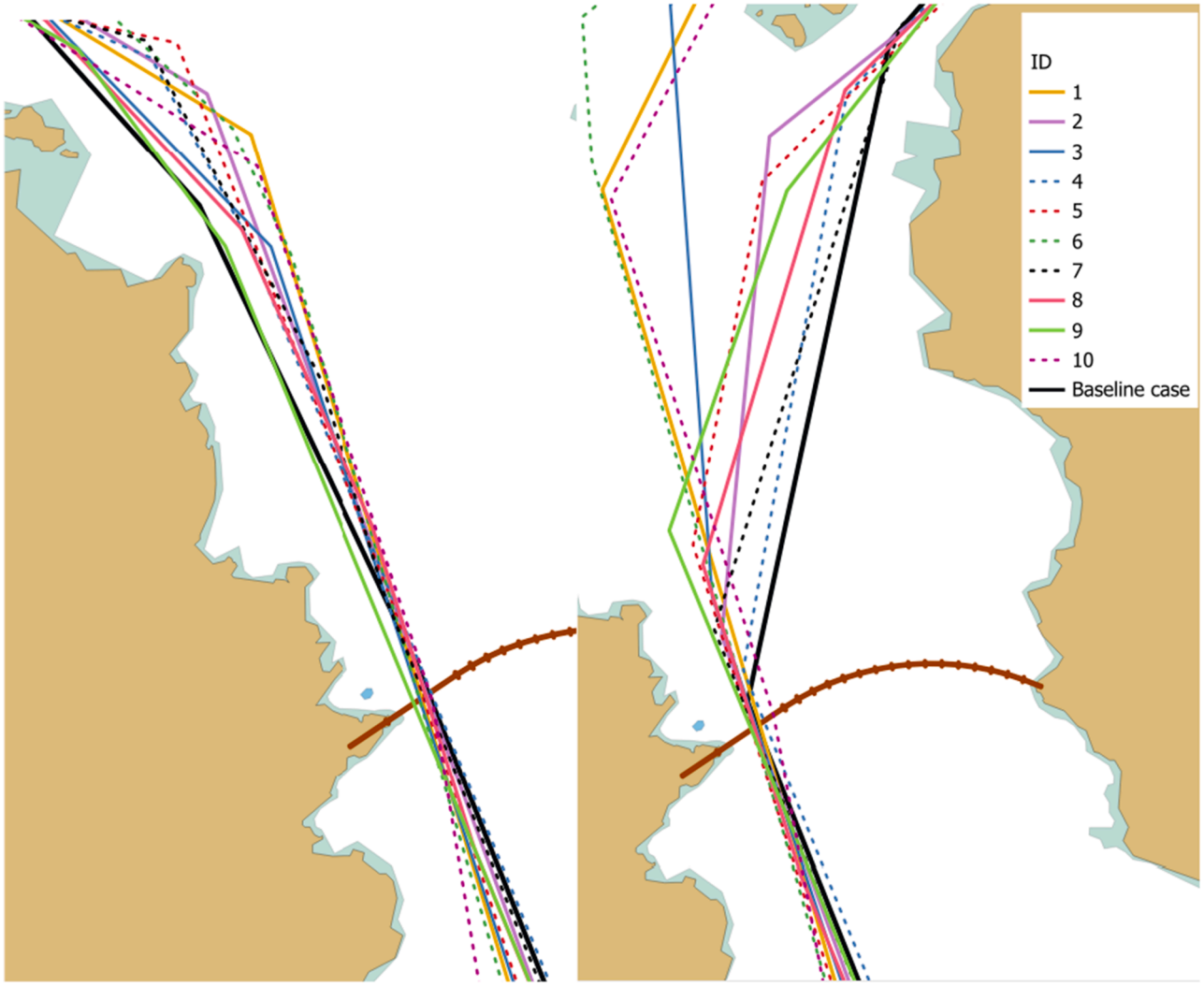

Fig. 15. The baseline case, routes 2 (left) and 3 (right) and the 10 experts' alteration of these routes.

and length of legs that are included in the model, but it usually takes several hours. The computation of probabilities in IWRAP Mk2 can be computed in less than a few minutes if the model can be computed in RAM memory. However, large models with detailed bathymetry might take several hours to compute in IWRAP Mk2. Although the ships run on autopilot in STAPS, it is important that the user ensures that ships manoeuvre as general ship traffic, which is a time-consuming task. Additionally, capturing of local failure statistics requires some time. Based on this, it is suggested that IWRAP Mk2 is a good starting model for the early design and analysis of case studies. However, STAPS enables the possibility to replay any allision that occurred in a simulation in real-time. This increases the understanding of why and how the allision occurred and thereby what mitigation actions would best reduce the accident probability. This also enables a better possibility to analyse the consequences of the allisions. The following conclusions are based on this second case study:

- IWRAP Mk2 limitations and the issues found in Case Study 1 seemed to have a minor impact on the results in a larger study.
- IWRAP Mk2 is a good initial model to determine maritime risks.
- The STAPS tool is designed to be agile and reasonable and thereby a good model to evaluate risk control options or specify specific events.
- Both models are sensitive to the layout and failure duration/repair time, making these parameters important to consider.

Since the route layout in Case Study 2 was found to have a major impact on the accident probability, it was further investigated in a separate analysis. According to Rong et al. [65,66], it is possible to predict where a ship will navigate in an existing routing system; however, it is more challenging when the routing system changes [67]. The design of the layout (how the ship routes are modelled) is a source of uncertainty that relates to the analyst's assumptions and experience. To quantify this sensitivity, five experts on maritime risk assessment employed at the Research Institutes of Sweden (RISE) and five international experts from different European countries were invited to a route layout benchmark study applied to the baseline scenario in Case Study 2. The experts worked independently, and they were given the same basic information regarding the AIS ship traffic data, the topology in the area and the bridge layout. Fig. 15 presents a summary of the participants' suggestions on the coordinates of the two routes 2 and 3.

Since there is no "correct way" of modelling how future traffic will navigate when a bridge has been built, the experts used their experience to define future routes. Both IWRAP Mk2 and STAPS were run with the experts' coordinates to quantify how route geometry affected allision probability (the IWRAP Mk2 models also included LEG 20 from Scenario 2.1). Further, all simulations were run with the same settings as Scenario 2.1. The results from the 10 experts' routes, including Scenario 2.1, are presented in Table 10.

As illustrated with the results of this sensitivity study presented in Table 10, how the future routes may look has a large impact on the expected number of allisions, from 2800 to 9400 in IWRAP Mk2 (average 4354) and from 619 to 17,216 in STAPS (average 3710). The route suggestion from participant 7 caused a large number of allisions, which were caused by the failure missed turning point and a waypoint close to the bridge. The low number of accidents with the route suggestions from participants 1 and 5 was derived from layouts without routes pointing towards the bridge. This indicates that the way future routes may look like is important. Therefore, future studies are suggested to investigate this topic further and to make recommendations on how to predict future routes that could be included in these types of probability assessments.

The real-world example of Dali hitting the Francis Scott Key Bridge in Baltimore [12] highlights an issue with Pedersen's categorisation. Since Dali was without propulsion, it should, in one aspect, be categorised as a drifting accident (Pedersen's accident category IV). However, due to its higher speed, it could also be categorised as a category I event. However, Dali was travelling in the normal route until the failure occurred, making it difficult to account for, while setting up a wide enough distribution to include it as a category I event. The STAPS model captures this accident by simulating the failure itself. The increased fidelity in the representation of failures reduces the model output uncertainty, which might otherwise be a source of additional conservatism [68].

IWRAP Mk2 is based on accidents, while STAPS is based on failures. The increased model fidelity level and the use of a model based on failures enable the addition of new failure modes caused by new advancements in the maritime domain, such as E-navigation and fully autonomous surface ships [42], which have different requirements for equipment degradation [69]. These advancements and rapid climate changes introduce new types of hazards (and possibly failure nodes) like rough ice and long distances in the Artic [70,71], and in ports [72]. The failure probabilities and durations in STAPS are based on AIS data. In future research other types of root causes could be included [36,43].

With regards to the risk of accidents, neither the IWRAP Mk2 nor STAPS model can assess the impact of accidents; however, a BiLSTM-CNN-RF model could make a rough estimate of the consequences [73], or this can be analysed in detail with analytic models like [74,75] or finite element models like [76–80]. Future studies are suggested to investigate how consequence modelling could be combined with probability models to develop risk models.

6. Conclusions

In this paper, two quantitative risk models, IWRAP Mk2 and STAPS, analysed ship-bridge allisions in two separate case studies, allowing a further analysis of the pros and cons of the respective models. The first case study focused on detailed differences between the two models, mainly how the implementation of hydrodynamic effects and ship geometry affected the assessments. The second case study had a more holistic view while studying the differences between the models in a real-world scenario.

Both case studies showed that IWRAP Mk2 estimated a higher probability of allisions compared to the STAPS estimations. In the first case study, this increase of accident probability was caused by the lack of hydrodynamic calculations in IWRAP Mk2, and in the second case study, it was caused by the low level of fidelity with regards to failure modelling. In this paper, it is shown that by increasing the failure model fidelity, it is possible to reduce the model uncertainty and thereby reduce the predicted accident probability.

The sensitivity analysis of route layout in Case Study 2 revealed that this modelling has a significant impact on accident probability, highlighting the importance of accurately predicting future ship routes. The variability in expert predictions emphasises the uncertainty inherent in modelling future traffic patterns, especially when routing systems change due to physical changes. Future studies should focus on developing methodologies to better predict future route layouts, which could enhance the accuracy of probability assessments for ship-bridge allisions.

In summary, both models are good for conducting probability

Table 10
Number of expected allisions with the layouts given by the 10 experts using $Y_{rep} = 10^6$ in STAPS and during 1000,000 years in IWRAP Mk2.

Model	Scenario 2.1	1	2	3	4	5	6	7	8	9	10
IWRAP Mk2	6310	2800	3300	6200	3700	3400	3300	5200	3700	2600	9400
STAPS	1435	665	1112	4254	2955	619	2889	17,216	2110	1539	3745

assessments. The IWRAP Mk2 software runs the analysis faster compared to STAPS by omitting hydrodynamics; while this might have an effect in a detailed analysis, in general it is deemed to be good enough. The major difference between the models is the fidelity of failure modelling: IWRAP Mk2 uses input derived from accidents, whereas STAPS uses real-world failures as input. IWRAP Mk2 is faster to run and is recommended to use in the early design phases. However, while executing the detail design, defining the accidental load case and studying risk mitigating actions on bridge design, fairway design and ship operation, it is recommended to use STAPS.

Beyond the specific context of ship-bridge allisions, the probabilistic models and risk assessment techniques developed in this study have broader applications in reliability engineering and system safety. Engineering models that currently use statistical methods to estimate accident probabilities could be adapted to simulate events more accurately. Future research could apply these methods in various fields, such as aerospace, automotive, and civil engineering. By focusing on specific events rather than general models, this study aims to advance reliability analysis and design, ultimately supporting the development of more resilient engineering systems.

CRediT authorship contribution statement

Axel Hörteborn: Writing – review & editing, Writing – original draft, Visualization, Validation, Software, Methodology, Investigation, Funding acquisition, Formal analysis, Data curation, Conceptualization. **Jonas W. Ringsberg:** Writing – review & editing, Writing – original draft, Supervision, Methodology, Formal analysis, Conceptualization. **Olov Lundbäck:** Writing – review & editing, Supervision, Software, Methodology. **Wengang Mao:** Writing – review & editing, Writing – original draft, Supervision, Conceptualization.

Declaration of competing interest

The authors declare the following financial interests/personal relationships which may be considered as potential competing interests:

Axel Hoerteborn reports financial support was provided by Swedish Transport Administration. Axel Hoerteborn reports financial support was provided by Norwegian Public Roads Administration. Jonas Ringsberg reports financial support was provided by Norwegian Public Roads Administration. Wengang Mao reports financial support was provided by Norwegian Public Roads Administration. If there are other authors, they declare that they have no known competing financial interests or personal relationships that could have appeared to influence the work reported in this paper.

Appendix

Table A1.

Table A1
Summary of relevant parameters that the user of the IWRAP Mk2 model provides. The presented values are used both in IWRAP Mk2 and STAPS in Case Study 1. Default values in IWRAP Mk2 are indicated with *.

Type of parameters	Name, abbreviation	Example value
Drift-related parameters	Blackout frequency, F_b	0.75 per year*
	Anchoring probability, P_{anchor}	70 %*
	Max anchor depth	7 times ship draught*
	Minimum distance to ground	2 times ship length*
	Repair time, function or distribution, $Pr_{l,o}$	$1 - e^{-1.05 \times t_{ddrift,l,o}^{0.9}}$ (A-1)
	Drift directions, Pdr_{dir}	[12.5 %, 12.5 %, 12.5 %, 12.5 %, 12.5 %, 12.5 %, 12.5 %, 12.5 %] *
	Drift speed, v_d	1 knot*
Bathymetry	Geometry	Polygon ((−1 −1, 1 0, 1 1, −1 1, −1 −1))
	Depth	100 meters
Structures	Structure – Geometry	Polygon ((0.033316 0.033108, 0.033316 0.033557, 0.042314 0.033558, 0.042314 0.033108, 0.033316 0.033108))
	Height	10 meters*
Leg information	Waypoint	WP1: Point (0.01636 0.033352) WP2: Point (0.01638 0.042306)
	Leg, l	From WP1–WP2
	Leg extension	50,000 meters*
	Lateral distribution	Uniform distribution [0, 1]
Traffic information (per ship category)	Ship frequency, $N_{l,sc}$	1000 ships/year
	Average ship speed, S_{sc}	15 knots
	Draught	12 meters
	Height	15 meters
Causation factor	Grounding—Powered	1.6×10^{-4}*
	Grounding—Drifting	1*
	Allision—Powered, Pc_p	1.6×10^{-4}*
	Allision—Drifting, Pc_d	1*
	Mean time between checks, t_m	180 s*

Data availability

Data will be made available on request.

References

[1] Thieme CA, Utne IB, Haugen S. Assessing ship risk model applicability to Marine Autonomous Surface Ships. Ocean Eng 2018;165:140–54. https://doi.org/10.1016/j.oceaneng.2018.07.040.

[2] Bhardwaj U, Teixeira AP. Guedes soares C. Probabilistic analysis of basic causes of vessel–Platform allision accidents. J Mar Sci Eng 2024;12:390. https://doi.org/10.3390/jmse12030390.

[3] Yu Q, Liu K, Yang Z, Wang H, Yang Z. Geometrical risk evaluation of the collisions between ships and offshore installations using rule-based Bayesian reasoning. Reliab Eng Syst Saf 2021;210:107474. https://doi.org/10.1016/j.ress.2021.107474.

[4] UNCTAD. Review of maritime transport 2021. Geneva: United Nations Publications; 2021.

[5] Antão P, Sun S, Teixeira AP, Soares CG. Quantitative assessment of ship collision risk influencing factors from worldwide accident and fleet data. Reliab Eng Syst Saf 2023;234:109166.

[6] Kaptan M, Uğurlu Ö, Wang J. The effect of nonconformities encountered in the use of technology on the occurrence of collision, contact and grounding accidents. Reliab Eng Syst Saf 2021;215:107886.

[7] Sánchez-Beaskoetxea J, Basterretxea-Iribar I, Sotés I, Machado M, de las MM. Human error in marine accidents: is the crew normally to blame? Marit Transport Res 2021;2:100016. https://doi.org/10.1016/j.martra.2021.100016.

[8] Gan L, Gao Z, Zhang X, Xu Y, Liu RW, Xie C, et al. Graph neural networks enabled accident causation prediction for maritime vessel traffic. Reliab Eng Syst Saf 2025;257:110804. https://doi.org/10.1016/j.ress.2025.110804.

[9] Li H, Çelik C, Bashir M, Zou L, Yang Z. Incorporation of a global perspective into data-driven analysis of maritime collision accident risk. Reliab Eng Syst Saf 2024;249:110187. https://doi.org/10.1016/j.ress.2024.110187.

[10] Zhang WZ, Pan J, Sanchez JC, Li XB, Xu MC. Review on the protective technologies of bridge against vessel collision. Thin-Walled Struct 2024;201:112013. https://doi.org/10.1016/j.tws.2024.112013.

[11] NTSB NTSB. Contact of containership Dali with the Francis Scott Key bridge and subsequent bridge collapse. 2024.

[12] Bradsher K. Recent bridge collapses raise questions about modern shipping. The New York Times; 2024.

[13] Fujii Y, Oshima R, Yamanouchi H, Mizuki N. Some factors affecting the frequency of accidents in marine traffic: i-the diameter of evasion for crossing encounters, II-the probability of stranding, III-the effect of darkness of the probability of collision and stranding. J Navigat 1974;27:239–47.

[14] Macduff T. The probability of vessel collisions. Ocean Ind 1974;9:144–8.

[15] Čorić M, Mandžuka S, Gudelj A, Lušić Z. Quantitative ship collision frequency estimation models: a review. J Mar Sci Eng 2021;9:533.

[16] BS-EN. BS En 1991-1-7: 2006. Eurocode 1: actions on structures, Part 1-7: General actions - Accidental actions. 2006.

[17] AASHTO. Guide specifications and commentary for vessel collision design of highway bridges. 2nd ed. U.S.: American Association of State Highway and Transportation Officials (AASHTO); 2009.

[18] Mazurek J, Lu L, Krata P, Montewka J, Krata H, Kujala P. An updated method identifying collision-prone locations for ships. A case study for oil tankers navigating in the Gulf of Finland. Reliab Eng Syst Saf 2022;217:108024.

[19] Murray B, Perera LP. An AIS-based deep learning framework for regional ship behavior prediction. Reliab Eng Syst Saf 2021;215:107819. https://doi.org/10.1016/j.ress.2021.107819.

[20] Sun L, Zhang Q, Ma G, Zhang T. Analysis of ship collision damage by combining Monte Carlo simulation and the artificial neural network approach. Ships Offshore Struct 2017;12:S21–30. https://doi.org/10.1080/17445302.2016.1258759.

[21] Zhang M, Montewka J, Manderbacka T, Kujala P, Hirdaris S. A big data analytics method for the evaluation of ship-ship collision risk reflecting hydrometeorological conditions. Reliab Eng Syst Saf 2021;213:107674.

[22] Zhang M, Conti F, Sourne HL, Vassalos D, Kujala P, Lindroth D, et al. A method for the direct assessment of ship collision damage and flooding risk in real conditions. Ocean Eng 2021;237:109605. https://doi.org/10.1016/j.oceaneng.2021.109605.

[23] Engberg PC. IWRAP Mk2 v5.3.0 manual. GateHouse A/S: IALA; 2017.

[24] Friis-Hansen P. Basic modelling principles for prediction of collision and grounding frequencies. 2008.

[25] Rawson A, Brito M, Sabeur Z, Tran-Thanh L. From conventional to machine learning methods for maritime riskassessment. Int J Mar Navigat Saf Sea Transport 2021;15.

[26] Jaeyong OH, Park S, Kwon O-S. Advanced navigation aids system based on augmented reality. Int J E-Navigat Marit Economy 2016;5:21–31.

[27] Ylitalo J. Modelling marine accident frequency. Alto University School of Science and Technology Faculty of Information and Natural Science; 2010.

[28] Pedersen PT. Collision and grounding mechanics. Copenhagen, Denmark: Danish Society of Naval Architecture and Marine Engineering; 1995. p. 125–57. vol. 1.

[29] Hörteborn A. Allision modelling in IWRAP MK II–a verification and sensitivity study. Advances in the collision and grounding of ships and offshore structures. CRC Press; 2024. p. 51–8.

[30] Son W-J, Cho I-S. Optimal maritime traffic width for passing offshore wind farms based on ship collision probability. Ocean Eng 2024;313:119498. https://doi.org/10.1016/j.oceaneng.2024.119498.

[31] Goerlandt F, Kujala P. Traffic simulation based ship collision probability modeling. Reliab Eng Syst Saf 2011;96:91–107. https://doi.org/10.1016/j.ress.2010.09.003.

[32] Ulusçu ÖS, Özbaş B, Altıok T, Or İ. Risk analysis of the vessel traffic in the strait of Istanbul. Risk Analysis 2009;29:1454–72. https://doi.org/10.1111/j.1539-6924.2009.01287.x.

[33] van Dorp JR, Merrick JRW. On a risk management analysis of oil spill risk using maritime transportation system simulation. Ann Oper Res 2011;187:249–77. https://doi.org/10.1007/s10479-009-0678-1.

[34] Munim ZH, Sørli MA, Kim H, Alon I. Predicting maritime accident risk using Automated Machine Learning. Reliab Eng Syst Saf 2024;248:110148. https://doi.org/10.1016/j.ress.2024.110148.

[35] Kretschmann L. Leading indicators and maritime safety: predicting future risk with a machine learning approach. J Shipp Trade 2020;5:19. https://doi.org/10.1186/s41072-020-00071-1.

[36] Zhang M, Taimuri G, Zhang J, Zhang D, Yan X, Kujala P, et al. Systems driven intelligent decision support methods for ship collision and grounding prevention: present status, possible solutions, and challenges. Reliab Eng Syst Saf 2025;253:110489. https://doi.org/10.1016/j.ress.2024.110489.

[37] Fan S, Yang Z. Accident data-driven human fatigue analysis in maritime transport using machine learning. Reliab Eng Syst Saf 2024;241:109675. https://doi.org/10.1016/j.ress.2023.109675.

[38] Rong H, Teixeira AP. Guedes Soares C. A framework for ship abnormal behaviour detection and classification using AIS data. Reliab Eng Syst Saf 2024;247:110105. https://doi.org/10.1016/j.ress.2024.110105.

[39] Korupoju AK, Kapadia V, Vilwathilakam AS, Samanta A. Ship collision risk evaluation using AIS and weather data through fuzzy logic and deep learning. Ocean Eng 2025;318:120116. https://doi.org/10.1016/j.oceaneng.2024.120116.

[40] Xue J, Yang P, Wang Z, Li Q, Hu H. Cause analysis and management strategies for ship accidents: a bayesian decision support model. Ocean Eng 2025;320:120291. https://doi.org/10.1016/j.oceaneng.2025.120291.

[41] Zhang W, Zhang Y, Zhang C. Research on risk assessment of maritime autonomous surface ships based on catastrophe theory. Reliab Eng Syst Saf 2024;244:109946. https://doi.org/10.1016/j.ress.2024.109946.

[42] Shiokari M, Itoh H, Yuzui T, Ishimura E, Miyake R, Kudo J, et al. Structure model-based hazard identification method for autonomous ships. Reliab Eng Syst Saf 2024;247:110046. https://doi.org/10.1016/j.ress.2024.110046.

[43] Tao J, Liu Z, Wang X, Cao Y, Zhang M, Loughney S, et al. Hazard identification and risk analysis of maritime autonomous surface ships: a systematic review and future directions. Ocean Eng 2024;307:118174. https://doi.org/10.1016/j.oceaneng.2024.118174.

[44] Baldauf M, Benedict K. Full mission and fast time simulation for ship handling training. Seaways: The Nautical Institute; 2018. p. 6–10.

[45] Bąk A, Gucma S, Przywarty M. Models of navigation risk used in restricted areas. Safety of navigation in restricted areas: methods of risk estimation and analysis. Cham: Springer Nature Switzerland; 2024. p. 57–97. https://doi.org/10.1007/978-3-031-49532-8_2.

[46] Kong M-C, Roh M-I. A method for implementing a ship navigation simulator for the generation and utilization of virtual data. Int J Naval Architect Ocean Eng 2024;16:100604. https://doi.org/10.1016/j.ijnaoe.2024.100604.

[47] Ma Y, Liu Q, Yang L, He M. Recognition of marine navigators' workload based on eye movement features using bridge simulation. Saf Sci 2024;178:106607. https://doi.org/10.1016/j.ssci.2024.106607.

[48] Hörteborn A, Ringsberg JW. A method for risk analysis of ship collisions with stationary infrastructure using AIS data and a ship manoeuvring simulator. Ocean Eng 2021;235:109396. https://doi.org/10.1016/j.oceaneng.2021.109396.

[49] Pedersen PT, Chen J, Zhu L. Design of bridges against ship collisions. Mar Struct 2020;74:102810. https://doi.org/10.1016/j.marstruc.2020.102810.

[50] ITU-R. Technical characteristics for an automatic identification system using time division multiple access in the vhf maritime mobile frequency band. Geneva: International Telecommunication Union; 2014.

[51] Guo S, Bolbot V, Valdez Banda O. An adaptive trajectory compression and feature preservation method for maritime traffic analysis. Ocean Eng 2024;312:119189. https://doi.org/10.1016/j.oceaneng.2024.119189.

[52] Hörteborn A, Eidem ME. Probability of active navigational failures. submitted to J Navigat 2025.

[53] Ozturk U, Cicek K. Individual collision risk assessment in ship navigation: a systematic literature review. Ocean Eng 2019;180:130–43. https://doi.org/10.1016/j.oceaneng.2019.03.042.

[54] Luo W, Li X. Measures to diminish the parameter drift in the modeling of ship manoeuvring using system identification. Appl Ocean Res 2017;67:9–20. https://doi.org/10.1016/j.apor.2017.06.008.

[55] sspasweden. PySim. Github 2020. https://github.com/sspasweden/pysim (Accessed 13 June 2023).

[56] Harris CR, Millman KJ, van der Walt SJ, Gommers R, Virtanen P, Cournapeau D, et al. Array programming with NumPy. Nature 2020;585:357–62. https://doi.org/10.1038/s41586-020-2649-2.

[57] Karlsson M, Rasmussen FM, Frisk L, Ennemark F. Verification of ship collision frequency model. Ship Collision Analysis; 1998. p. 117–21.

[58] Norwegian Meteorological Institute. Catalog. 2022. https://thredds.met.no/thredds/catalog/obs/mast-svv-e39/catalog.html (Accessed 15 August 2022).

[59] Knutsen Ø, Stefanakos C. Ferry-free E39 - Currents. Trondheim, Norway: Sintef Ocean; 2022.

[60] Limpert E, Stahel WA, Abbt M. Log-normal distributions across the sciences: keys and clues: on the charms of statistics, and how mechanical models resembling gambling machines offer a link to a handy way to characterize log-normal distributions, which can provide deeper insight into variability and probability—Normal or log-normal: that is the question. Bioscience 2001;51:341–52.

[61] Crestelo Moreno F, Roca Gonzalez J, Suardíaz Muro J, García Maza JA. Relationship between human factors and a safe performance of vessel traffic

service operators: a systematic qualitative-based review in maritime safety. Saf Sci 2022;155:105892. https://doi.org/10.1016/j.ssci.2022.105892.
[62] Vegvesen Statens. Håndbok N400 Bruprosjektering - Eurokodeutgave. Håndbok N400 bruprosjektering - eurokodeutgave, Statens Vegvesen. 2014.
[63] Zhou Y, Daamen W, Vellinga T, Hoogendoorn SP. Impacts of wind and current on ship behavior in ports and waterways: a quantitative analysis based on AIS data. Ocean Eng 2020;213:107774. https://doi.org/10.1016/j.oceaneng.2020.107774.
[64] Ricci A, Vasaturo R, Blocken B. An integrated tool to improve the safety of seaports and waterways under strong wind conditions. J Wind Eng Ind Aerodyn 2023;234:105327. https://doi.org/10.1016/j.jweia.2023.105327.
[65] Rong H, Teixeira AP. Guedes Soares C. Maritime traffic probabilistic prediction based on ship motion pattern extraction. Reliab Eng Syst Saf 2022;217:108061. https://doi.org/10.1016/j.ress.2021.108061.
[66] Rong H, Teixeira AP, Soares CG. Ship abnormal behaviour detection off the continental coast of Portugal. Trends Marit Technol Eng 2022:143–50.
[67] Lee J-S, Lee M-S, Cho I-S. Changes in maritime traffic patterns according to installation of floating LiDAR using spatial analysis. IEEE Access 2023;11:74784–95. https://doi.org/10.1109/ACCESS.2023.3296795.
[68] Aven T. On the use of conservatism in risk assessments. Reliab Eng Syst Saf 2016;146:33–8. https://doi.org/10.1016/j.ress.2015.10.011.
[69] Luo X, Guo L, Bai X, Li Y, Zan Y, Luo J. A multi-phase mission success evaluation approach for maritime autonomous surface ships considering equipment performance degradation and system composition changes. Reliab Eng Syst Saf 2025;254:110604. https://doi.org/10.1016/j.ress.2024.110604.
[70] Kandel R, Baroud H. A data-driven risk assessment of Arctic maritime incidents: using machine learning to predict incident types and identify risk factors. Reliab Eng Syst Saf 2024;243:109779. https://doi.org/10.1016/j.ress.2023.109779.
[71] Yu Y, Liu K, Fu S, Chen J. Framework for process risk analysis of maritime accidents based on resilience theory: a case study of grounding accidents in Arctic waters. Reliab Eng Syst Saf 2024;249:110202. https://doi.org/10.1016/j.ress.2024.110202.
[72] Lucio D, Lara JL, Tomás A, Losada IJ. Probabilistic assessment of climate-related impacts and risks in ports. Reliab Eng Syst Saf 2024;251:110333. https://doi.org/10.1016/j.ress.2024.110333.
[73] Qiao W, Huang E, Zhang M, Ma X, Liu D. Risk influencing factors on the consequence of waterborne transportation accidents in China (2013–2023) based on data-driven machine learning. Reliab Eng Syst Saf 2025;257:110829. https://doi.org/10.1016/j.ress.2025.110829.
[74] Zhang S, Villavicencio R, Zhu L, Pedersen PT. Impact mechanics of ship collisions and validations with experimental results. Mar Struct 2017;52:69–81.
[75] Zhang S, Villavicencio R, Zhu L, Pedersen PT. Ship collision damage assessment and validation with experiments and numerical simulations. Mar Struct 2019;63:239–56.
[76] Ladeira I, Márquez L, Echeverry S, Le Sourne H, Rigo P. Review of methods to assess the structural response of offshore wind turbines subjected to ship impacts. Ships Offshore Struct 2023;18:755–74. https://doi.org/10.1080/17445302.2022.2072583.
[77] Ringsberg JW, Amdahl J, Chen BQ, Cho S-R, Ehlers S, Hu Z, et al. MARSTRUCT benchmark study on nonlinear FE simulation of an experiment of an indenter impact with a ship side-shell structure. Mar Struct 2018;59:142–57.
[78] Sha Y, Amdahl J, Dørum C. Local and global responses of a floating bridge under ship–Girder collisions. J Offshore Mech Arct Eng 2019;141. https://doi.org/10.1115/1.4041992.
[79] Sha Y, Amdahl J. A simplified analytical method for predictions of ship deckhouse collision loads on steel bridge girders. Ships Offshore Struct 2019;14:121–34. https://doi.org/10.1080/17445302.2018.1560881.
[80] Yu Z, Amdahl J. A review of structural responses and design of offshore tubular structures subjected to ship impacts. Ocean Eng 2018;154:177–203. https://doi.org/10.1016/j.oceaneng.2018.02.009.